



**FRANCISCA RODRIGUES DA PIEDADE** **MODELOS 3D HUMANIZADOS PARA O ESTUDO DE DOENÇAS PULMONARES**

**TAKING ADVANTAGE OF 3D HUMANIZED IN VITRO MODELS TO STUDY PULMONARY DISEASES**



**FRANCISCA RODRIGUES DA MODELOS 3D HUMANIZADOS PARA O ESTUDO DE DOENÇAS  
PIEIDADE PULMONARES**

**TAKING ADVANTAGE OF 3D HUMANIZED IN VITRO MODELS  
TO STUDY PULMONARY DISEASES**

Dissertação apresentada à Universidade de Aveiro para cumprimento dos requisitos necessários à obtenção do grau de Mestre em Bioquímica, realizada sob a orientação científica da Doutora Catarina de Almeida Custódio, Investigadora Pós-Doutorada do Departamento de Química da Universidade de Aveiro e coorientação da Doutora Catarina Rodrigues de Almeida, Professora Auxiliar do Departamento de Ciências Médicas da Universidade de Aveiro.

À minha mãe e irmã,

## **O júri**

Presidente

**Professor Doutor Carlos Pedro Fontes Oliveira**  
Professor Auxiliar do Departamento de Química da Universidade de Aveiro

Arguente

**Professora Doutora Sílvia Joana Bidarra dos Santos Lourenço**  
Investigadora Júnir, i3S (Inst de Investigação e Inovação em Saúde) e INEB (Instituto de Engenharia Biomédica), Universidade do Porto

Orientador

**Doutora Catarina de Almeida Custódio**  
Investigadora Pós-Doutorada do Departamento de Química da Universidade de Aveiro

## **Agradecimentos**

Em primeiro lugar gostaria de agradecer à Doutora Catarina Custódio pela orientação científica e pela oportunidade de realizar este projeto. Foi um período atípico por razões que nos ultrapassam, mas aprendi muito e estou grata por toda a simpatia, disponibilidade e saber que me transmitiu.

Quero agradecer à Doutora Catarina Almeida pela orientação, interesse e dedicação, e por ter sempre uma atitude positiva em relação ao trabalho.

Um grande obrigado à Sara, que durante todo o percurso me ensinou, aconselhou, e alegrou quando as coisas corriam menos bem. Foste incansável e tornaste todo o percurso mais fácil e divertido!

Obrigada à Beatriz pela disponibilidade e apoio no laboratório, pela positividade e por ter sempre uma palavra amiga.

Agradeço com carinho à minha família e aos meus amigos, em especial à minha mãe e irmã, ao Steve e à Daniela, pelo vosso amor, empatia e paciência ao longo deste percurso e de todos os outros.

Ao Rafael, obrigada por teres caminhado ao meu lado nos últimos anos e por seres o apoio incondicional que és.

Aos membros do COMPASS Group e do Ibimed, obrigada pelo companheirismo e por me terem acolhido tão bem desde o primeiro dia.

**palavras-chave**

Fibrose Pulmonar, Doenças fibróticas, Matriz extracelular, Modelos 3D de pulmão, Lisados de plaquetas metacrilatados.

**resumo**

A fibrose pulmonar, que se caracteriza por cicatrização progressiva e irreversível do tecido pulmonar, culminando em falha pulmonar, é umas das principais causas de morte a nível mundial. Os mecanismos patológicos na gênese da fibrose pulmonar não são claros; as teorias atuais sugerem a ocorrência de uma cicatrização anormal em resposta a lesões pulmonares crônicas, nas quais os estímulos mecânicos e químicos do ambiente pulmonar induzem a ativação dos fibroblastos. As opções de tratamento atuais são muito limitadas, sendo o transplante pulmonar a única opção viável para pacientes em estágio final de fibrose. Plataformas tridimensionais (3D) de pulmão capazes de simular a função e estrutura pulmonares e as interações célula-célula e célula-matriz são, por isso, necessárias para compreender os mecanismos patológicos e os mediadores envolvidos no processo fibrótico. Dos vários biomateriais usados em engenharia de tecidos (ET), os hidrogéis têm ganho destaque: são redes poliméricas 3D que absorvem água, capazes de fornecer suporte mecânico às células e de permitir a difusão de nutrientes, metabólitos e oxigênio. São particularmente interessantes para estudar doenças pulmonares, uma vez que conseguem simular as propriedades mecânicas e viscoelásticas de tecidos moles como o pulmão. Os hidrogéis naturais são plataformas atrativas por serem biocompatíveis e bioativas. Plasma Rico em Plaquetas (PRP) e Lisados de Plaquetas (LP) humanos têm sido usados para criar hidrogéis, por serem uma fonte humana de fatores de crescimento (FC). No entanto, têm fracas propriedades mecânicas e são facilmente degradáveis. Os hidrogéis sintéticos não têm estas limitações, mas faltam-lhes sinais indutores de diferenciação, cruciais para o desenvolvimento dos tecidos. Hidrogéis à base de LP metacrilatados (LPM) foram recentemente propostos como plataformas bioquimicamente e biomecanicamente superiores para cultura de células. Neste trabalho, propomos estes hidrogéis autólogos e ricos em FC como uma plataforma 3D capaz de mimetizar o pulmão fibrótico. Os hidrogéis de LPM recapitularam a rigidez do pulmão fibrótico, e permitiram manter fibroblastos pulmonares viáveis durante pelo menos 7 dias em cultura. As células adotaram diferentes morfologias consoante a rigidez da matriz e induziram marcadas deformações nos hidrogéis de LPM, sugerindo que estas plataformas induziram um fenótipo fibrótico nos fibroblastos e que, por isso, mimetizam a remodelação patológica da matriz extracelular que ocorre na fibrose pulmonar.

**keywords**

Lung fibrosis, Fibrotic diseases, Extracellular matrix, 3D lung models, hydrogels, PLMA.

**abstract**

Pulmonary fibrosis, characterized by progressive and irreversible lung tissue stiffening resulting in organ failure, is a growing health problem and belongs to the major causes of death worldwide. The pathological mechanisms of lung fibrosis are not fully understood; current pathogenic theories assume an impaired wound healing response to chronic lung injuries, in which the mechanical and chemical stimuli from the lung environment induces fibroblast activation. Currently, therapeutic options are severely limited, and lung transplantation remains the only effective treatment for patients in end-stage fibrotic diseases. Complex tridimensional (3D) lung platforms able to accurately recapitulate function, structure, and cell and matrix interactions found in fibrotic lung tissue, are therefore necessary to provide the means for understanding the pathological mechanisms and mediators involved in the fibrotic process. Of the vast array of biomaterials that have been used for Tissue Engineering (TE) applications, a major enthusiasm has been developed towards hydrogels: 3D water-swollen polymeric networks, that provide mechanical support to cells and allow for the diffusion of nutrients, waste, and oxygen. Hydrogels are particularly interesting to study lung diseases as they recapitulate the mechanical and viscoelastic properties found in load-bearing soft tissues like the lung. Natural-based hydrogels are appealing platforms as they are inherently biocompatible and bioactive. Platelet-rich plasma (PRP) and human platelet lysates (PL) provide interesting materials to create hydrogels as they are a source for human-derived growth factors (GF). However, they present poor mechanical properties and are easily degraded. Synthetic-derived hydrogels do not face these limitations, but they lack differentiative cues required for tissue development. Human methacryloyl platelet lysates (PLMA)-based hydrogels have been proposed as a biochemical and biomechanical-superior platform for cell culture purposes. These autologous, GF-rich, platforms are herein proposed as reliable 3D platforms to model the fibrotic lung. PLMA hydrogels recapitulated the pathological stiffness of the fibrotic lung and supported the viability of lung fibroblasts cells for at least 7 days in culture. Cells adopted different morphologies as matrix stiffness changed and were able to induce matrix deformations in PLMA hydrogels, suggesting the feasibility of this scaffold to induce a profibrotic phenotype in fibroblasts in 3D, therefore recapitulating the pathological remodeling of lung fibrosis.





## Contents

List of tables .....	iii
List of figures .....	iv
Abbreviations .....	v
Preamble – Thesis organization .....	1
Chapter I .....	2
Taking advantage of 3D cell culture platforms to study lung development and pulmonary diseases* .....	2
Abstract .....	3
Pulmonary Fibrotic Diseases .....	4
3D Lung Models .....	5
Scaffolds .....	6
Polymeric-based scaffolds .....	7
Decellularized Scaffolds .....	9
PCLT .....	11
Lung Spheroids .....	14
Lung Organoids .....	15
Lung-on-a-chip .....	16
Conclusions .....	18
Bibliography: .....	20
Chapter II .....	31
Aims .....	31
Bibliography: .....	33
Chapter III .....	34
Platelet lysates-based hydrogels for 3D lung modeling .....	34
Introduction .....	35

<b>Cellular and biochemical mechanisms in fibrosis .....</b>	<b>36</b>
<b>Platelet-based biomaterials as humanized 3D models .....</b>	<b>37</b>
<b>PLMA-based hydrogels to model the fibrotic lung .....</b>	<b>39</b>
<b>Experimental Section.....</b>	<b>40</b>
<b>Synthesis of Methacryloyl Platelet Lysates (PLMA) .....</b>	<b>40</b>
<b>Preparation of PLMA hydrogels.....</b>	<b>41</b>
<b>Cells culture experiments.....</b>	<b>42</b>
<b>Biological performance of PLMA-based hydrogels .....</b>	<b>43</b>
Cell viability: LIVE/DEAD Assay .....	43
Cells morphology: Immunostaining.....	43
<b>Compressive Mechanical Testing.....</b>	<b>44</b>
<b>Sircol™ Soluble Collagen Assay.....</b>	<b>44</b>
<b>Statistical analysis .....</b>	<b>45</b>
<b>Results and Discussion.....</b>	<b>45</b>
<b>Bibliography:.....</b>	<b>52</b>
<b>Chapter IV.....</b>	<b>60</b>
<b>Conclusions and Future Perspectives .....</b>	<b>60</b>
<b>Conclusions and Future Perspectives .....</b>	<b>61</b>

## List of tables

<b>Table 1.</b> Summary of the uses, advantages, and limitations of different 3D lung models. ....	19
--	----

## List of figures

<b>Figure 1.</b> Schematic representation of the currently available 3D lung models and their properties. ....	6
<b>Figure 2.</b> Illustrative representation of lung decellularization and recellularization processes. ....	10
<b>Figure 3.</b> Illustrative representation of the procedure to generate PCLS. ....	12
<b>Figure 4.</b> Illustrative representation of PLMA preparation. ....	41
<b>Figure 5.</b> IMR90 cell line at passage 7. ....	42
<b>Figure 6.</b> Illustrative representation of IMR90 encapsulation within PLMA100 hydrogels. A: cell count and centrifugation. B: Resuspension of cell pellet in PLMA100 solution. C: PLMA100 cell suspension pipetting into the plate. D: Photopolymerization of PLMA100 hydrogels with UV light for 60s and addition of growth medium. ....	43
<b>Figure 7.</b> Illustrative representation of collagen quantification using Sircol Assay Kit. A: Standards (values expressed in $\mu\text{g}$ ) and sample preparation; B: Microplate reading at 555nm. ....	45
<b>Figure 8.</b> PLMA hydrogels before <b>(A)</b> and after <b>(B)</b> mechanical compression, and Young Modulus of PLMA100 and PLMA200 hydrogels at 10%, 15%, and 20% w/v <b>(C)</b> . Statistical analysis through unpaired t-test showed significant differences ( $*p < 0.05$ ) between the analyzed groups ( $n=3$ ). ...	46
<b>Figure 9.</b> Representative fluorescence images for IMR90 upon LIVE/DEAD staining at 1, 3, and 7 days of culture in <b>(A)</b> PLMA100 and <b>(B)</b> PLMA200 hydrogels at 10%, 15%, and 20% w/v. Images are representative of 8 independent experiments. ....	48
<b>Figure 10.</b> Representative fluorescence images for DAPI (blue) and phalloidin (red) staining to label the nuclei and actin cytoskeleton of IMR90 cells at 7 days of culture in PLMA100 10%, 15%, and 20% hydrogels. Images are representative of 2 independent experiments. ....	49
<b>Figure 11.</b> Young Modulus of PLMA100 hydrogels at 10%, 15%, and 20% w/v after 3d of TGF- $\beta$ stimulation <b>(A)</b> , and representative images of IMR90 fibroblasts encapsulated in PLMA100 hydrogels at day 0 <b>(B)</b> and 1 <b>(C)</b> day of culture. Statistical analysis through unpaired t-test showed no significant differences ( $*P < 0.05$ ) between the analyzed groups ( $n=2$ ). ....	49
<b>Figure 12.</b> Collagen quantification in recovered culture medium. IMR90 fibroblasts were cultured embedded in PLMA hydrogels and supplemented with ascorbic acid and TGF- $\beta$ for 3d. Soluble collagen was extracted and measured using Sircol Assay kit. Preliminary results ( $n=1$ ). ....	51

## Abbreviations

<b>2D</b>	Two-dimensional
<b>3D</b>	Three-dimensional
<b>AA</b>	Ascorbic Acid
<b>AEC</b>	Alveolar Epithelial Cells
<b>CHAPS</b>	3-[(3-cholamidopropyl)dimethylammonio]-1-propanesulfonate
<b>COPD</b>	Chronic Obstructive Pulmonary Diseases
<b>ECM</b>	Extracellular Matrix
<b>EHS</b>	Engelbreth-Holm-Swarm
<b>EMT</b>	Epithelial-Mesenchymal Transition
<b>FBS</b>	Fetal Bovine Serum
<b>FG</b>	Fibrin Glue
<b>bFGF</b>	Basic Fibroblast Growth Factor
<b>GF</b>	Growth Factor
<b>HPS</b>	Hermansky-Pudlak Syndrome
<b>hPSC</b>	Human Pluripotent Stem Cells
<b>HPSIP</b>	HPS-associated Interstitial Pneumonia
<b>IIP</b>	Idiopathic Interstitial Pneumonia
<b>ILD</b>	Interstitial Lung Diseases
<b>IPF</b>	Idiopathic Pulmonary Fibrosis
<b>LAP</b>	Latency-associated Peptide
<b>MA</b>	Methacrylic Anhydride
<b>MMP</b>	Matrix Metalloproteinase
<b>MSC</b>	Mesenchymal Stem Cells
<b>mTOR</b>	Mammalian Target of Rapamycin

<b>NSCLC</b>	Non-Small Cell Lung Cancer
<b>PBS</b>	Phosphate buffered saline
<b>PC</b>	Platelet Concentrate
<b>PCLT</b>	Precision Cut Lung Tissue
<b>PDS</b>	Patient-derived tumor Spheroids
<b>PEG</b>	Polyethylene glycol
<b>PG</b>	Platelet Gel
<b>PGA</b>	Polyglycolic Acid
<b>PI</b>	Propidium Iodide
<b>PL</b>	Platelet Lysates
<b>PLG</b>	Platelet lysate-gel
<b>PLMA</b>	Methacryloyl Platelet Lysates
<b>PPP</b>	Platelet-poor Plasma
<b>PRGF</b>	Plasma-Rich in Growth Factor
<b>PRP</b>	Platelet-rich plasma
<b>ROS</b>	Reactive Oxygen Species
<b>TE</b>	Tissue Engineering
<b>TGF-<math>\beta</math></b>	Transforming growth factor- $\beta$
<b>T<math>\beta</math>RI</b>	Transmembrane type I receptor
<b>T<math>\beta</math>RII</b>	Transmembrane type II receptor
<b><math>\alpha</math>-SMA</b>	$\alpha$ -smooth muscle actin

## **Preamble – Thesis organization**

This thesis presents a discussion and the development of novel 3D platforms to study pulmonary diseases. Thus, the first chapter of this thesis reviews previous studies of 3D lung models, addressing scaffold-based lung models, precision cut lung tissue slices (PCLT), lung spheroids and organoids, and also lung-on-a-chip. Then, Chapter II summarizes the aims of the thesis, and Chapter III presents a new model for lung fibrosis, based on platelet lysates-based hydrogels. This chapter includes an Introduction, a detailed description of the experimental work performed, finalizing with the Results obtained and its Discussion. Finally, Chapter IV provides the Conclusions and Future Perspectives.

# Chapter I

## **Taking advantage of 3D cell culture platforms to study lung development and pulmonary diseases\***

\* This chapter was adapted from the following publication: Piedade F, Mano JF, Custódio CA, Almeida CR. "Taking advantage of 3D cell culture platforms to study lung development and pulmonary diseases" (under review)



# Taking advantage of 3D cell culture platforms to study lung development and pulmonary diseases

Francisca Piedade<sup>1</sup>, João F. Mano<sup>1</sup>, Catarina A. Custódio<sup>\*1</sup>, Catarina R. Almeida<sup>\*2</sup>

<sup>1</sup> Department of Chemistry, CICECO, University of Aveiro, Campus Universitário de Santiago, 3810-193 Aveiro, Portugal

<sup>2</sup> iBiMED – Institute of Biomedicine, Department of Medical Sciences, University of Aveiro, 3810-193 Aveiro, Portugal

\*equal contribution

Co-corresponding authors:

Catarina R. Almeida, iBiMED – Institute of Biomedicine, Department of Medical Sciences, University of Aveiro, 3810 – 193 Aveiro, Portugal, telephone: +351 234 247 244, email: [cra@ua.pt](mailto:cra@ua.pt)

Catarina A. Custódio, Department of Chemistry, CICECO, University of Aveiro, Campus Universitário de Santiago, 3810 - 193 Aveiro, Portugal, telephone: +351 234 370 200, email: [catarinacustodio@ua.pt](mailto:catarinacustodio@ua.pt)

## Abstract

Pulmonary fibrosis consists of progressive and irreversible lung tissue stiffening that is typically associated with organ failure. This is a major health problem and a leading cause of death worldwide. The mainstays of current therapy for lung fibrosis rely on lung transplantation in end-stage fibrotic diseases. This is associated with severe limitations due to the shortage of organ donors and risks of rejection. Recent advances in 3D tissue engineering allowed the creation of complex 3D lung platforms that accurately recapitulate lung function, structure, and cell and matrix interactions, therefore providing the means for understanding the pathological mechanisms and mediators involved in the fibrotic process. In this perspective, this review discusses the most relevant 3D cell culture platforms to engineer lung models as well as their applications *in vitro*.


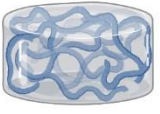

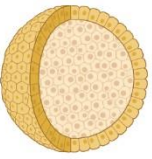

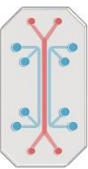
## Pulmonary Fibrotic Diseases

Lung fibrosis is characterized by progressive and irreversible loss of native lung architecture as normal healthy lung tissue is converted to scar tissue<sup>1</sup>. Scar formation compromises the normal lung function leading to disruption of proper gas exchange and ultimately causing death due to the collapse of the respiratory system<sup>2</sup>. Interstitial Lung Diseases (ILD) are a group of diffuse parenchymal lung conditions characterized by (1) chronic inflammation, with inflammatory cells persistence within the lung (mainly lymphocytes and macrophages) and exacerbated levels of pro-inflammatory, angiogenic, and fibrogenic cytokines, growth factors (GFs) and proteases<sup>3</sup>, and (2) varying degrees of lung fibrosis<sup>4</sup>. The remodeling of lung parenchyma that characterizes this group of fibrotic lung disorders occurs through the accumulation of extracellular matrix (ECM)<sup>5</sup>. The epidemiology of lung fibrotic diseases is difficult to estimate, as fibrosis often occurs with pulmonary and extrapulmonary comorbid conditions (e.g., lung cancer, respiratory infections, and cardiovascular disorders). Notwithstanding, many studies suggest that the prevalence of ILD is increasing worldwide<sup>6</sup>. Also, several studies reported the increased incidence and mortality associated with ILD<sup>7</sup>. For most patients, it is possible to identify an underlying trigger to these diseases. However, when the cause is unknown, they are diagnosed with idiopathic interstitial pneumonia (IIP). Idiopathic pulmonary fibrosis (IPF) is the most common and aggressive form of IIP, with 2–3 years of survival rate after diagnosis. While the key initiating triggers are still to be identified, evidence shows that lung fibrosis develops as an atypical response to lung injury leading to aberrant wound healing responses, epithelial apoptosis and senescence, dysregulated fibroblast activity, and transdifferentiation, excessive ECM deposition, and immune reactions<sup>8</sup>. Despite progress regarding the pathological mechanisms of pulmonary fibrosis, there are still many unmet needs and treatment options are still scarce. To date, many compounds have been tested as potential therapeutic drugs for fibrotic lung diseases. However, the multiple pathways and mediators involved in the fibrotic process, and the deficiency of robust drug screening platforms that more accurately predict patient's response, have limited the efficacy of current therapies<sup>9</sup>. For example, pirfenidone and nintedanib have been authorized for the treatment of pulmonary fibrosis<sup>10</sup>, but these drugs only slow disease progression and do not offer a cure or improve survival rate of patients. Furthermore, no clinically prognostic or predictive biomarker tests have been approved, making it difficult to guide patient care<sup>8</sup>. Considering the increasing global burden of fibrotic lung diseases<sup>11</sup>, additionally to the limited treatment options<sup>10</sup>, a better understanding of the disease mechanisms is crucial for the development of effective therapies. Complex models able

to accurately mimic native tissues could provide a better understanding of the disturbed signaling networks of fibrotic lung disease and help to discover and validate new potential therapies (**Table 1**).

### **3D Lung Models**

For many years, mammalian models have been indispensable for the understanding of lung physiology in health and disease, providing a bridge between patients and the laboratory<sup>12</sup>. However, ethical and safety concerns and the limited correlation existing between animal models and clinical trials<sup>13</sup>, have boosted the search for alternatives. Most of the current studies on pulmonary fibrotic lung diseases are based on two-dimensional (2D) cell culture substrates. Although very useful to obtain basic information related to cellular responses, cell cultures grown in tissue culture plates are not able to accurately recapitulate the complex and hierarchical organization of native lung tissue. *In vivo*, cells reside in a complex tridimensional (3D) environment, that exposes them to different GF gradients, mechanical cues, and polarities, and allows them to establish cell-cell and cell-ECM interactions<sup>14,15</sup>. Considering the shortage of donors of human lungs for research and the limitations of the previously referred models, the need for more tissue-like platforms emerged. Tissue engineering (TE) combines cells, 3D scaffolds, and specific biochemical signals that favor cell adhesion, growth, and differentiation to create functional 3D tissues<sup>16</sup>. Advances in TE techniques have already allowed the assembly of more physiologically and pathologically relevant 3D models of the human lung, and nowadays *in vitro* models of all the main parts of the respiratory tract are available<sup>17</sup>. These 3D models have revolutionized pulmonary research as they can mimic the complex lung environment and architecture, allowing researchers to better study cellular mechanisms, lung development, and responses of pulmonary tissue to ECM alterations as well to mechanical stimuli<sup>18</sup>. So far, the proposed 3D models include scaffolds (polymeric-based and decellularized organs or tissues), precision cut lung tissue slices (PCLT), lung spheroids, lung organoids, and lung-on-a-chip (**Figure 1**).

<b>3D LUNG MODELS</b> 	SCAFFOLD-BASED	POLYMERIC-BASED		<ul style="list-style-type: none"> <li>• Recapitulate the natural ECM;</li> <li>• Tunable mechanical properties;</li> <li>• Tunable cellular organization within the matrix;</li> <li>• Difficulties in oxygen and nutrient diffusion in the inner parts of the scaffold.</li> </ul>
	LUNG-DERIVED	PCLS		<ul style="list-style-type: none"> <li>• Maintenance of cellular organization;</li> <li>• Preservation of ECM structural and chemical integrity.</li> <li>• Physiological responses to stimuli;</li> <li>• Challenging technique.</li> </ul>
	SELF-ASSEMBLED	SPHEROID		<ul style="list-style-type: none"> <li>• Simple</li> <li>• Cancer modeling;</li> <li>• Low control over spheroid uniformity;</li> <li>• Long-term culture difficulties.</li> </ul>
		ORGANOID		<ul style="list-style-type: none"> <li>• Replicates developmental processes;</li> <li>• Represents human physiology;</li> <li>• Allows disease modelling;</li> <li>• Allows precision medicine (patient-derived organoids);</li> <li>• Low standardization.</li> </ul>
	LUNG-ON-A-CHIP			<ul style="list-style-type: none"> <li>• Replicates dynamic organ level processes, including cyclical strain breathing and shear stress due to blood flow;</li> <li>• Allows the integration of advanced imaging machinery.</li> </ul>

**Figure 1.** Schematic representation of the currently available 3D lung models and their properties.

## Scaffolds

Scaffolds refer to 3D porous structures that provide structural support for 3D cell adhesion, proliferation, and differentiation. The adequate selection of a scaffold is crucial for the successful development of lung tissue. The ideal scaffolding material for lung TE must provide the necessary support for cell growth and tissue development without compromising the elastic recoil of the tissue. Here, the 3D scaffolds typically used to engineer lung models were divided according to their source: i) 3D structures prepared from polymeric sources and ii) decellularized scaffolds isolated from native tissues. Both of them provide means of controlling engineered tissue architecture and mechanical properties, and they are designed to replicate tissue-specific microenvironments<sup>19</sup>.

## Polymeric-based scaffolds

The ECM is the natural niche of cells *in vivo*. Having this in mind, many studies have been focused on developing biomaterials that recapitulate the natural ECM and provide cells with a favorable microenvironment. Instead of inert structures, advanced biomimetic scaffolds provide cells with structural, mechanical, and biochemical cues that allow them to behave like their native counterparts<sup>20–22</sup>.

Hydrogels have been extensively used as scaffolds for TE applications. Due to their inherent features, they can recapitulate the mechanical and viscoelastic properties found in the human tissues, including load-bearing soft tissues like the lung. Hydrogels are 3D networks consisting of either physically or chemically crosslinked polymers with high water content and allow for the diffusion of nutrients, oxygen, waste, and soluble factors<sup>23,24</sup>. Additionally, they can be easily modified to improve their bioactivity, viscoelastic properties, and degradability<sup>25</sup>.

Hydrogels can be prepared from either natural or synthetic materials, offering a broad list of ECM-like scaffolds with multiple mechanical and chemical properties<sup>26</sup>. Natural-derived hydrogels for 3D cell culture are typically prepared using proteins and other ECM components, namely collagen, fibrin, hyaluronic acid, mixtures such as Matrigel, and also polymers obtained from other natural sources such as chitosan, alginate, or silk<sup>21,27–29</sup>. Naturally-derived hydrogels are appealing for biological applications as they are inherently biocompatible and bioactive, and also because they are a great source of endogenous factors, therefore promoting many cellular functions<sup>27</sup>. However, natural-based scaffolds present several boundaries including poor mechanical properties, limited control over their degradation rates and physicochemical properties, and also potential immunogenicity<sup>26,27,30</sup>.

A classic natural material to model the human lung is collagen and its derivatives<sup>27</sup>. Fibrillar collagens are the main protein component of the ECM of the lung (types I, II, III, V, and XI), providing structural integrity to the tissue<sup>31</sup>. Sugihara and colleagues reported the encapsulation of alveolar type II epithelial cells in a collagen hydrogel, which proliferated and formed alveolus-like luminal structures<sup>32</sup>. The 3D culture of fibroblasts in a hydrogel made of collagen type I has allowed researchers to investigate cell behaviors with the surrounding microenvironment and key aspects of this complex dynamic interaction<sup>33</sup>. It has been found that the level of  $\alpha$ -smooth muscle actin ( $\alpha$ -SMA) expression, a fibroblast contractile marker, was directly proportional to gel compliance, as stiff collagen-based materials promote increased expression of  $\alpha$ -SMA and integrin ( $\alpha$ 1,  $\beta$ 1), while collagen gels with lower compliance promote reduced expression of those markers<sup>34</sup>. The weak

mechanical properties of collagen constructs limit its use to non-load-bearing applications, although there are already strategies to improve its stiffness, such as crosslinking<sup>35-37</sup>, mechanical compression<sup>38</sup>, and the combination of collagen with other ECM proteins<sup>39</sup>. Besides fibrillar collagens, large elastic fibers and proteoglycans are also an important component of the pulmonary ECM<sup>40,41</sup>. On one hand, fibrillar collagens provide good tensile strength although low elasticity, while large elastic fibers are characterized by little tensile strength but high elasticity, providing the lung with the required compliance and intrinsic recoil<sup>41</sup>. Elastic fibers comprise of two major components: elastin, crosslinked in their inner core, and 10-15 nm-sized microfibrils, in their periphery<sup>40,41</sup>. Elastin plays a crucial role in the mechanical properties of the lung, acting synergistically with collagen in the biomechanical behavior of lung tissue. A collagen-elastin scaffold has been prepared to produce a superior material able to mimic the mechanical properties of the alveolar wall<sup>39</sup>. The addition of soluble elastin to the collagen hydrogels increased their stiffness, overcoming the limited mechanical strength of pure collagen hydrogels. Additionally, human lung fibroblasts seeded in the hybrid scaffolds resulted in a Young's modulus matching the known value (5 kPa) for the pulmonary alveoli wall<sup>39</sup>.

Another gold standard scaffold material for 3D cell culture is Matrigel<sup>42</sup>. Matrigel consists of a mixture of proteins secreted by Engelbreth-Holm-Swarm (EHS) mouse sarcoma cells rich in laminin, GFs, entactin/nidogen, type IV collagen, and heparan sulfate proteoglycan<sup>43</sup>. Wu *et al.* cultured human bronchial epithelial cells on Matrigel, and showed that those cells expressed specific markers for polarized acinar cells, suggesting their differentiation, but did not express a ciliated cell marker<sup>44</sup>. Although Matrigel cultured bronchial acini produced bronchial epithelial cells devoid of cilia, these cells displayed glandular hyperplasia and could, therefore, be used to model cystic fibrosis and chronic obstructive pulmonary diseases (COPD). Despite its excellent biocompatibility and cytocompatibility, the fact that Matrigel derives from murine sarcoma makes this platform unsuitable for translational applications.

Several biocompatible and biodegradable synthetic polymers have also been developed for TE applications. Synthetic scaffolds can provide great mechanical support, and their physicochemical properties can be easily tuned to control cell function<sup>26</sup>. Anseth *et al.* reported the synthesis of photodegradable polyethylene glycol (PEG) hydrogels containing a photodegradable functionality, a nitrobenzyl ether-derived moiety that allows the gel degradation upon light exposure<sup>45</sup>. This feature allows for on-demand alterations in macroscopic properties such as hydrogel stiffness, water content, or complete hydrogel degradation. Additionally, synthetic hydrogels show low

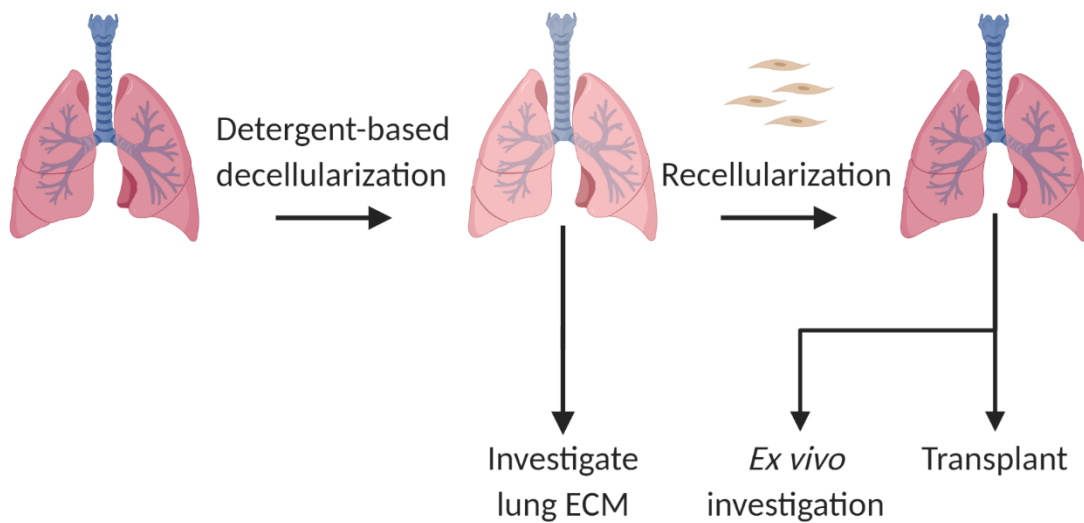
potential for immunogenic reactions and can be consistently reproduced on a large scale<sup>46</sup>. However, they lack biological cues, which are crucial to engineering tissue-like structures without supplementation with bioactive components and GFs.

A polyglycolic acid (PGA)-based scaffold has been developed and seeded with lung progenitor cells that could differentiate into multiple cell types, expressing lung-specific markers, and the use of PGA facilitated tissue formation *in vitro*<sup>47</sup>. Despite the promising *in vitro* results to engineering lung tissue, further *in vivo* tests have shown that PGA induces a foreign body response, resulting in an inflammatory reaction that interfered with tissue growth<sup>47</sup>. Furthermore, biodegradable Poly(L-lactic acid) and Poly(lactic-co-glycolic acid) hydrogels have been seeded with primary fetal pulmonary isolates<sup>48</sup>. Infiltration and proliferation of the cells were evident in both matrices, but no tissue-specific differentiation occurred. These results corroborate the hypothesis that typically, synthetic scaffolds offer great mechanical support, but lack the essential biochemical cues necessary for engineering lung tissue, even with the addition of specific biomolecules to the medium<sup>48</sup>.

The development of advanced hydrogels for 3D cell culture is challenging, requiring the control of the physical and chemical properties of the material. There are several factors to take into consideration when developing a functional ECM mimic: hydrogels' mechanical properties, presence of adhesive ligand and GFs to support the formation of tissue-like constructs, transport, and degradation kinetics, and degradation products. Ultimately, the objective is to engineer an advanced scaffold that gathers the advantages of natural and synthetic materials in order to fulfill the cellular needs.

## **Decellularized Scaffolds**

Decellularization is a process that involves the removal of the cellular content from a tissue or organ while preserving its ECM with the original 3D matrix and structure of the tissue/organ<sup>49</sup>. Several methods for lung decellularization have been described<sup>50-52</sup> but so far there is no consensus on the best method. Most of these methods are detergent-based and use a combination of both ionic and nonionic detergents that lyse and remove the cellular components while preserving the structural and chemical integrity of the ECM<sup>49</sup> (**Figure 2**). Successful decellularization is obtained when no cellular and nuclear content is detected by routine histological analysis, the amount of DNA is lower than 50ng/mg of dry tissue, and fragments of DNA run on a gel are above 200 bp<sup>53</sup>.



**Figure 2.** Illustrative representation of lung decellularization and recellularization processes.

After cell and cell-derived molecules removal, lung microarchitecture and lung mechanical dynamics may be directly altered as lung mechanics is directly impacted by the surrounding matrix and connective tissue composition<sup>54</sup>. The chosen detergent and decellularization approach will therefore directly impact the mechanical properties of the decellularized scaffold<sup>55</sup>. Among the different protocols that have already been used to decellularize tissues, the zwitterionic detergent 3-[(3-cholamidopropyl)dimethylammonio]-1-propanesulfonate (CHAPS) efficiently removed the cellular components with minimal loss of ECM proteins such as elastin, collagen, and laminin<sup>56–59</sup>. However, there is no consensus on the best method yet, and some authors believe that Triton X-100 and SDC work better in protecting the ECM structure and removing cellular components than methods using SDS or CHAPS detergent<sup>49</sup>. Decellularized lung matrices can be further solubilized and used to design scaffolds through electrospinning<sup>60</sup> or to create 3D hydrogels through an acidic pepsin digestion<sup>61–63</sup>.

Initially, the main goal of decellularization technologies was to overcome the limited availability of organ donors and provide an advanced scaffold that would not trigger an immune reaction in the transplant recipient<sup>64</sup>. However, translational studies are still very limited and decellularized lung matrices have been mostly used for investigational purposes. They have been used to investigate the substructure of the lung<sup>65</sup>, and to gain insights about ECM, its chemical composition, and mechanical features<sup>49</sup>. Also, decellularized lung matrices have been recolonized with recipient cells, providing an essential platform for expanding our knowledge regarding pulmonary diseases<sup>64</sup>. Booth *et al.* used acellular human normal and fibrotic lungs as an *in vitro* model to study how ECM affects fibroblast myodifferentiation in a disease-specific manner<sup>66</sup>. The normal and fibrotic human



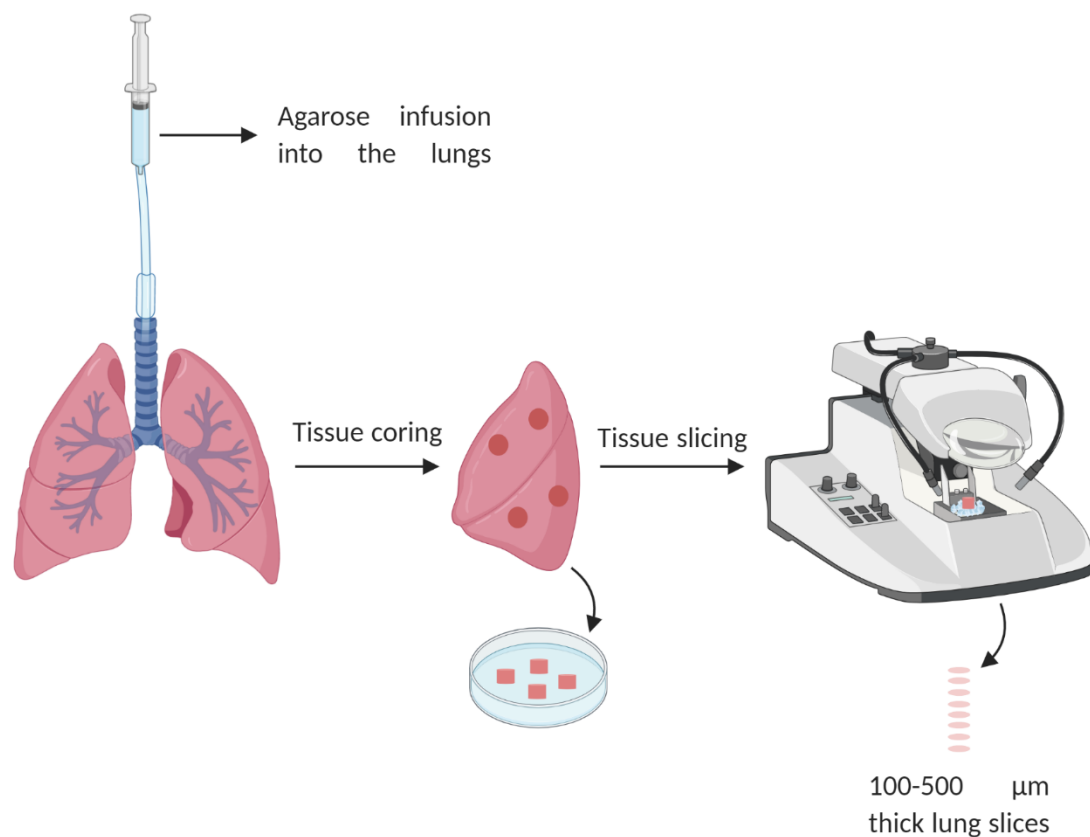
lungs were decellularized and seeded with healthy human fibroblasts. Fibrotic lung matrices retained their pathological stiffness, and induced cellular activation to myofibroblasts, with increased production of  $\alpha$ -SMA, a feature typically seen in fibrotic tissue. These results suggest that the composition and mechanical function of the ECM is involved in disease progression. Additionally, transforming growth factor- $\beta$ 1 (TGF- $\beta$ 1) bioactivity was similar in normal and fibrotic matrices suggesting a TGF- $\beta$ 1 independent fibroblast myodifferentiation mechanism. Although not able to identify the signaling pathway responsible for fibroblast myodifferentiation in IPF, this *in vitro* model provided insights about the mechanical contribution of the ECM to IPF pathogenesis. In another study, primary lung fibroblasts obtained from either IPF or healthy lungs were seeded in decellularized lungs from healthy and IPF patients<sup>67</sup>. It was found that the antifibrotic miR-29 family was downregulated by fibrotic ECM, evidencing that the scaffold source had a higher influence on the expression of fibrotic genes, compared to cell origin. Also, emphysematous lungs obtained from murine and human COPD have been decellularized, with the lungs retaining their pathological features<sup>68</sup>. When recellularized with immortalized epithelial cells, decellularized emphysematous lung scaffolds did not sustain cell proliferation and survival, compared to those recellularized on healthy lung scaffolds<sup>68</sup>. Also, cell survival was reduced in emphysematous lungs from older mice. Later, the authors found out that these changes in epithelial cell proliferation and survival were related to decreased laminin expression in scaffolds obtained from aged mice<sup>69</sup>. These results suggest that the age of the donor of the decellularized lung would probably have a significant impact on ECM composition, and must therefore be considered in lung bioengineering.

These 3D lung models are a valuable tool to gain insights into ECM composition, cell-ECM interactions, and cellular behavior on diseased decellularized lungs. Although decellularization protocols still need to be improved, these scaffolds can provide a means to understand lung biology, pathogenic mechanisms of lung diseases, and help identify alternative treatment options that focus on cell-matrix interactions.

## **PCLT**

Precision cut lung tissue slices (PCLT) or *ex vivo* lung tissue refers to lung slices used for *in vitro* research of tissues with cells. In contrast with decellularized matrices, lung slices are prepared from fresh tissue, from lung cadavers, surgical resections, or explanted lungs<sup>70</sup>. For soft tissues such as the lung, slices can be technically challenging to obtain. However, this was surpassed by the standardized infusion of the lungs with heated liquid agarose, which maintains the lung inflated,

and thus avoids that the tissue collapses during slicing<sup>71-72</sup>(**Figure 3**). PCLT can be maintained in culture with an appropriate culture medium. Many articles have reported that PCLT remain viable only for one to six days in culture<sup>73-75</sup>. In an attempt to overcome that, Temann et al. reported the optimization of the culture medium by supplementation with essential nutrients and antibiotics<sup>76</sup>. In this study, cultured PCLT retained their viability, metabolic activity, tissue structural integrity, and cell populations, and responded to stimulation with lipopolysaccharide up to 14 days<sup>76</sup>. Also, Bailey et al. encapsulated PCLT in hydrogels based in poly(ethylene glycol), and these platforms could be maintained in culture for 21 days, which is a significant culture time increase compared to PCLT floating in media<sup>77</sup>.



**Figure 3.** Illustrative representation of the procedure to generate PCLT.

The main advantage of using PCLT is the maintenance of the tissue's architecture as they retain its structure, immune cell populations, and connective tissue. Also, PCLT maintain the ratios of the different cell populations, as well as the interactions between cell-cell and cell-matrix. Another advantage is that PCLT might be rapidly, reproducibly, and quantitatively produced, and subsequently analyzed using high throughput technology<sup>78</sup>. However, due to the variability between different regions within the lung, specific cell types can vary between slices. Regardless,

PCLT have demonstrated to be a useful tool to correlate cellular function with organ physiology as they have been used to study responses to stimuli such as contraction of the airways and the immune response<sup>76,79,80</sup>. Thus, this “mini lung” has been used as a model of lung diseases, and as a tool for toxicology studies, drug screening, and potential therapeutic targets<sup>81-85</sup>. For example, PCLT obtained from healthy and asthmatic patients showed different responses to stimulation, including bronchoconstriction and hyperresponsiveness, in diseased lungs<sup>86</sup>. These results are in agreement with previous animal-based evidence<sup>87,88</sup>, demonstrating the ability of PCLT to mimic lung physiology. PCLT have thus been used to model suppression of asthma symptoms, such as airway constriction, with glucocorticoids in combination with bronchodilators<sup>89,90</sup>.

Also, PCLT exposed to cadmium chloride and TGF- $\beta$ 1 demonstrated pathohistological changes similar to the histological patterns seen in early lung fibrogenesis, such as an increase in profibrotic genes, myofibroblasts activation leading to higher ECM deposition, and changes in protein patterns<sup>82,91</sup>. Recently, non-IPF/ILD human PCLT were exposed to a profibrotic cocktail (with TGF- $\beta$ , PDGF-AB, TNF- $\alpha$ , and LPA), which resulted in fibrotic-like changes in the lung tissue, such as higher production of profibrotic and proinflammatory cytokines, ECM secretion, deposition, and alveolar epithelium injury<sup>92</sup>. Murine and human PCLS treated with a similar profibrotic cocktail were used to evaluate nintedanib and pirfenidone effect, and results showed that nintedanib increased the levels of alveolar epithelial markers that were inhibited with the fibrotic treatment<sup>93</sup>. The same fibrosis-induced PCLS were used to investigate the effect of EP300 inhibition in IPF treatment, and results show that this histone deacetylase inhibition resulted in attenuation of fibrosis hallmarks in the fibrosis-induced PCLT<sup>94</sup>.

Remarkably, we demonstrated that EP300 inhibition reduced fibrotic hallmarks in vitro using primary fibroblasts from Ctrl and IPF patients, in vivo using the bleomycin mouse model, and ex vivo using PCLS

Dysfunctional PI3K/ mammalian target of rapamycin (mTOR) signaling is associated with abnormal proliferation in IPF and cancer and Mercer et al. used PCLS to establish a dosing range of GSK2126458, an inhibitor of PI3K/mTOR<sup>85</sup>. By targeting PI3K/mTOR, the expression of procollagen 1 amino-terminal peptide was significantly reduced, therefore suggesting GSK2126458 as a new therapeutic drug for IPF treatment<sup>85</sup>. Following this work, Woodcock and coworkers found that the TGF- $\beta$ 1 stimulated collagen synthesis signaled via PI3K/mTOR is exerted through human lung fibroblasts<sup>95</sup>.

Overall, PCLT can contribute to comprehend the pathomechanisms of lung diseases, provide insight into novel therapeutic targets, and be useful to study the efficacy and safety of therapeutic drugs. Heterogeneity between lung samples, lung regions, and even lung slices might cause difficulties in data interpretation. Furthermore, PCLT have limited viability, therefore restricting long term investigations. Also, they are unable to mimic an immune response as they cannot recruit non-resident immune cells. Lastly, these models are intricate and expensive to implement, and appropriate lung tissue is not always available.

## Lung Spheroids

Sutherland *et al.* first developed multicellular spheroid cultures in 1970, in an attempt to simulate human tumors and study how they respond to radiotherapy<sup>96,97</sup>. Ever since spheroid cultures have been implemented with several different cells. Spheroids are very well-characterized models of solid tumors and drug screening due to their simple and reproducible preparation, and also because they maintain the functional phenotype of human tumor cells<sup>98</sup>. Spheroids are clusters of cells that self-assemble, where intercellular interactions overlap cell-surface interactions<sup>99</sup>. Spheroids do not need any scaffolds for assembly, relying on the contact between the cells and the ECM deposition that occurs spontaneously<sup>100</sup>. There are four main fabrication methods reported in the literature to create spheroids: (i) agitation-based techniques<sup>101</sup>, (ii) hanging drop technique, (iii) liquid overlay technique<sup>102</sup>, and lastly (iv) microfluidics<sup>103</sup>. Additionally, there are a great variety of commercial products such as Perfecta3D<sup>®</sup> hanging drop plates and GravityPLUS<sup>™</sup> plates, for the production of spheroids under controlled and reproducible conditions. Spheroid culture models have many advantages when compared to monolayer cultures as they develop oxygen, nutrients, soluble factors, and metabolic waste gradients, thus favoring the growth of various cell populations, with the round geometry optimizing intercellular and cell-ECM interactions<sup>104</sup>. Considering its similarities with *in vivo* tumors, spheroids have been mainly used for the study of lung tumor biology and drug screening<sup>99,105–107</sup>, being also very useful to complement patient individual drug treatment as they enable the use of primary cells obtained from the patient tissue.

Patient-derived tumor spheroids (PDS) were recently cultured from advanced non-small cell lung cancer (NSCLC) patient samples to recapitulate the cytological features and markers of NSCLC and their utility as a drug screening platform. By surgically resecting tissue from NSCLC chemotherapy-naive patients, cells obtained from the tissue were cultured to form PDS with about 500 $\mu$ m<sup>108</sup>. Also, a human NSCLC cell line (H1299) was cultured in spheroids to test the feasibility for drug screening

purposes and as a model for lung cancer biology. The cytotoxicity of cisplatin was investigated and results showed higher values of IC50 in the spheroids in comparison to monolayer cultures, highlighting the potential of these tumor spheroids for clinical application: the IC50 of the PDS could be used to estimate the chemotherapy response of an individual patient<sup>108</sup>.

Although able to create a physiologically relevant 3D tumor tissue model, these sphere-like culture systems fail to recapitulate organ function, as they lack vasculature. Also, because spheroids use tumor derived-cells, immortalized cell lines, and cells obtained from patients' xenografts, it is hard to control the rate of cell growth, and therefore the size of the cell aggregate<sup>104</sup>.

## **Lung Organoids**

'Lung organoids' are structures that self-assemble and are generated from lung progenitor cells<sup>109</sup>. Organoids are a powerful tool for basic and translational research and have already been generated to replicate lung structures, including bronchi/bronchioles and alveoli<sup>110-112</sup>.

Lung organoids have been obtained from various epithelial cells from the lung, such as alveolar epithelial cells (AECs) or human pluripotent stem cells (hPSCs). AEC are particularly relevant to study respiratory disorders, namely IPF, as the structure and function of the alveoli is affected in this type of disease. Therefore, studying the biology of these cells, as well as their niche might provide important clues regarding pathological disease mechanisms. To generate lung organoids, however, not only alveolar cells are required. These cells need support and clues for proper proliferation and differentiation. The proximity between AEC and mesenchymal cells has already been shown to be crucial for organotypic alveolar epithelium development in mice<sup>113</sup>. The Clevers lab formed human airway organoids derived from NSCLC patient's lung tissue<sup>114</sup>. These lung organoids were easily grown from small amounts of materials obtained from patients, which is useful as it fights the shortage of available lung tissue for TE application. Furthermore, these organoids derived from diseased patients are amenable to medium-throughput drug screening, which shows their potential use in personalized medicine<sup>114</sup>.

Protocols for hPSC-derived organoids have also been established, including embryonic stem cells and iPSCs<sup>115,116</sup>. In 2014, single bronchioalveolar stem cells were cultured with endothelial cells as support and differentiated *in vitro* into different epithelial lineages<sup>117</sup>. The authors identified an important mechanism that regulates differentiation in the lung: the BMP4-NFATc1-TSP1 signaling axis. This work elucidates that lung stem cells can be differentiated into specific lineages upon

manipulation of the cells' microenvironment, which might be a promising therapeutic approach against lung diseases<sup>117</sup>. Considering the unclear IPF, efforts have been made to decode this disease. Hermansky-Pudlak syndrome (HPS)-associated interstitial pneumonia (HPSIP), a clinical entity similar to IPF, is associated with recessive mutations in genes implicated in HPS. Strikoudis *et al.*, investigated if the introduction of HPS mutations would promote fibrotic changes in lung organoids<sup>118</sup>. Results showed that lung organoids derived from epithelial stem cells with mutated HPS exhibited a similar phenotype as HPSIP patients with corresponding mutations, demonstrating the potential of this model to recapitulate important features of the disease. Furthermore, there was a higher expression of IL-11 in epithelial cells from fibrotic organoids with mutant HPS; the similarity in the expression signatures of organoid and lung samples from patients with IPF indicates that this model might be a powerful tool in identifying IPF pathogenic mechanisms<sup>118</sup>.

There are still technical challenges to obtain organoids similar to *in vivo* tissue, with the same complexity and maturity, while retaining the reproducibility that is required for screening (as most of them still lack key cell types and vasculature). Notwithstanding, organoids hold great potential to model human lung and lung diseases, as a tool for the identification of novel drug targets and as a preclinical tool for innovative therapeutics.

## **Lung-on-a-chip**

An organ-on-a-chip is a small platform that includes a microchamber and a continuously perfused hollow microchannel able to recapitulate the organ vascular system and tissue microenvironment<sup>104</sup>. 3D cell culture in microfluidics aims to mimic the complexity of living tissues and this technology has already been adapted to model various regions of the human lung, such as the airways and alveoli.

Huh *et al.* has reported a microfluidic system mimicking the human alveolar-capillary interface<sup>119</sup>. Human AECs were cultured in one of the sides of the ECM-coated membrane and endothelial cells from the lung vasculature on the opposite side<sup>119</sup>. This membrane was placed in a microfluidic device that supplied both sides of the membrane with nutrients, allowing for the compartmentalization of the system, until cells grew to confluence<sup>119</sup>. The epithelial side was then exposed to air, mimicking the air-liquid interface typical of a real lung<sup>119</sup>. Besides the air-liquid interface, this device also recapitulated the breathing movements through vacuum pumps that applied cyclic mechanical stretch to the alveolar-capillary interface<sup>119</sup>. The epithelial cells in the microfluidic device had higher production of surfactant, as well as increased electrical resistance,

and an improved function as a molecular barrier<sup>119</sup>. This system has also been applied to model the induction of pulmonary edema by drugs<sup>120</sup>. Furthermore, a multichambered culture system has allowed analysis of the kinetics of cellular responses to environmental agents<sup>121</sup>. This system integrated permeable filter supports with human primary airway epithelial cells at the air-liquid interface perfused by basal media, mimicking the interstitial flow that happens *in vivo*. An automated fraction collector allowed analysis of the kinetics of IL-8 release upon exposure to grass pollen. The amount of IL-8 released was significantly superior compared to static culture conditions, which might be related to a negative feedback mechanism. In this system, released IL-8 was constantly removed, unlike static conditions, where it accumulates over time. The IL-8 kinetic profile was undetectable in static conditions while the microfluidic culture enabled a time-dependent IL-8 release analysis in response to grass pollen exposure. This microfluidic culture system allowed for the exchange of fluids and mediators, namely IL-8, therefore showing that microfluidic devices replicate the dynamic interstitial flow that happens *in vivo* better than static culture conditions<sup>121</sup>. A lung-on-a-chip with a "breathing" ultra-thin membrane has been used to analyze how cyclic mechanical stress impacts alveolar wound repair<sup>122</sup>. A549 lung alveolar epithelial cells were cultured on PDMS membranes coated with fibronectin and then seeded on the apical side of the alveolar membrane that is deflected through a microdiaphragm mimicking the mechanical strain of breathing. By scratching the cell layer a wound was created without tearing apart the PDMS membrane. It was found that wound closure was quicker in static conditions and that adding recombinant human hepatic GF accelerated closure in both dynamic and static conditions. And as previously shown, cyclic mechanical stretch leads to a reduction in the capacity of the epithelium to close the wound<sup>123</sup>. The authors also reported that regardless of mechanical stretch, epithelial wound healing was reduced on a porous membrane compared to a non-porous membrane, which might be related to the fact that in a porous membrane the space between the ECM and the cells weakens the cell-ECM interactions and slows down cell migration, therefore impairing wound healing. This breathing-lung-on-a-chip emulated key features of the lung alveolar environment such as the air-liquid interface that lets cells receive their nutrients through the basolateral side while being in contact with air on the apical side. However, this membrane lacks ECM, and thus Zamprogno and colleagues developed a lung-on-a-chip with a collagen and elastin membrane that can be stretched and alveoli that can be sized, which is a far better representation of the alveolar compartment<sup>124</sup>.

Organ-on-a-chip platforms accurately replicate dynamic organ level processes, intercellular and cell-matrix interactions, and are suitable for evaluating effects of drugs, particulates, pathogens, or

other stimuli important in clinical applications. Additionally, these lung microsystems might be integrated with other organ-biomimetic models in one single device to mimic exchanges between various organs and therefore replicate the whole body's physiology<sup>125</sup>.

## **Conclusions**

In recent years there has been great progress in developing advanced 3D culture systems able to accurately reproduce the physiologic parameters within both normal and diseased tissues, overcoming the limitations of traditional 2D plate culture systems. These systems provide the means to identify disease-specific pathological mechanisms, and in the future might be used as preclinical tools for drug screening. Although animal models are important tools in drug development and preclinical toxicity testing, advanced 3D lung models could provide a reliable alternative with a more accurate prediction of clinical outcomes. Additionally, these models could help identify drug-induced complications and adverse side effects before the clinical trials. Importantly, the use of ECM-derived and decellularized scaffolds allows the development of personalized therapeutic strategies.



**Table 1.** Summary of the uses, advantages, and limitations of different 3D lung models.

3D models	Uses	Advantages	Limitations	Ref.
<b>Natural scaffolds</b>	<ul style="list-style-type: none"> <li>• As a drug delivery system</li> <li>• To study cell-ECM interactions</li> <li>• Study of induced fibrosis pathological mechanisms</li> <li>• Study of cell-cell and cell-ECM interaction</li> </ul>	<ul style="list-style-type: none"> <li>• Natural origin</li> <li>• Bioactivity and biocompatibility</li> <li>• Intrinsic structural resemblance with native ECM</li> </ul>	<ul style="list-style-type: none"> <li>• Cannot model long-term responses, undergoes degradation and contraction</li> <li>• Degradation kinetics hard to predict</li> <li>• Inconsistent compositions</li> <li>• Weak mechanical properties</li> <li>• Can cause immune responses</li> </ul>	20,39,126
<b>Synthetic scaffolds</b>		<ul style="list-style-type: none"> <li>• Low immune responses</li> <li>• Defined purity and reproducibility</li> <li>• Good mechanical properties</li> </ul>	<ul style="list-style-type: none"> <li>• Lack bioactive domains</li> <li>• Poor biocompatibility and bioactivity</li> </ul>	
<b>Decellularized scaffolds</b>	<ul style="list-style-type: none"> <li>• To study: <ul style="list-style-type: none"> <li>-The substructure of the lung;</li> <li>-Lung ECM (chemical composition and mechanical features)</li> <li>-Lung diseases, lung repair, and regeneration mechanisms</li> </ul> </li> <li>• Drug testing</li> </ul>	<ul style="list-style-type: none"> <li>• Preserves pre-existing arterial and venous vascular tree and bronchial network</li> <li>• Retains ECM protein composition</li> <li>• Cell-matrix interactions similar to <i>in vivo</i></li> <li>• Can be stored frozen</li> <li>• Long-term culture</li> <li>• Time-lapse live imaging</li> </ul>	<ul style="list-style-type: none"> <li>• Decellularization-related ECM loss</li> <li>• Access to lung samples</li> <li>• Poor protocol standardization</li> </ul>	49-127
<b>PCLS</b>	<ul style="list-style-type: none"> <li>• Study of short-term responses</li> <li>• Replication of native/diseased lung microenvironment</li> </ul>	<ul style="list-style-type: none"> <li>• Accurate cell-matrix, cell-cell interactions</li> <li>• Retain cellular and structural organization of the lung</li> <li>• Thickness, dimensional tunability</li> </ul>	<ul style="list-style-type: none"> <li>• Short-term (~5 days) investigation</li> <li>• Requires fresh live lung samples</li> <li>• Storage not possible</li> </ul>	70, 78, 128
<b>Spheroids</b>	<ul style="list-style-type: none"> <li>• Mostly for cancer research</li> <li>• Drug screening and toxicity testing</li> </ul>	<ul style="list-style-type: none"> <li>• Easy fabrication and Self-assembling</li> <li>• Replicate cell-cell, cell-matrix interactions</li> <li>• Allows co-culture of cells</li> <li>• Allows personalized disease modeling and treatment</li> </ul>	<ul style="list-style-type: none"> <li>• Variation in size</li> <li>• Difficult to observe via live imaging</li> <li>• Lack vasculature</li> <li>• Heterogeneities in drug penetration</li> </ul>	98-100, 104
<b>Organoids</b>	<ul style="list-style-type: none"> <li>• Basic and translational research</li> <li>• Drug screening and toxicity testing</li> </ul>	<ul style="list-style-type: none"> <li>• Self-assembling</li> <li>• Replicate cell-cell, cell-matrix interactions</li> <li>• Allows co-culture of cells</li> <li>• Allows for personalized disease modeling and treatment by using patient-derived cells</li> </ul>	<ul style="list-style-type: none"> <li>• Requires long-term culture</li> <li>• Technical challenges to produce complex organoids</li> <li>• Lack vasculature and perfusion</li> </ul>	114
<b>Lung-on-a-chip</b>	<ul style="list-style-type: none"> <li>• Drug screening and toxicity testing</li> <li>• Study of induced fibrosis pathological mechanisms under dynamic lung microenvironment</li> </ul>	<ul style="list-style-type: none"> <li>• Replicates cyclical strain breathing and shear stress due to blood flow</li> <li>• Allows for oxygen and nutrients gradients and removal of metabolic waste</li> <li>• Replicate cell-cell, cell-matrix interactions</li> <li>• Time-lapse live imaging</li> </ul>	<ul style="list-style-type: none"> <li>• Time-lapse live-cell imaging requires complex imaging equipment</li> </ul>	104, 129, 125

## Bibliography:

1. Wynn, T. A. Integrating mechanisms of pulmonary fibrosis. *J. Exp. Med.* **208**, 1339–1350 (2011).
2. Prof Luc aRicheldi, Harold R Collard & Mark G Jones. Idiopathic pulmonary fibrosis. **369**, 1941–1952 (2017).
3. Wynn, T. A. Common and unique mechanisms regulate fibrosis in various fibroproliferative diseases. *J Clin Invest* **117**, 524–529 (2007).
4. Bagnato, G. & Harari, S. Cellular interactions in the pathogenesis of interstitial lung diseases. *European Respiratory Review* **24**, 102–114 (2015).
5. David W. Waters *et al.* Fibroblast senescence in the pathology of idiopathic pulmonary fibrosis. **315**, 162–172 (2018).
6. Rivera-Ortega, P. & Molina-Molina, M. Interstitial Lung Diseases in Developing Countries. *Ann Glob Health* **85**, (2019).
7. Choi, W.-I., Park, S. H., Dauti, S., Park, B.-J. & Lee, C. W. Interstitial lung disease and risk of mortality: 11-year nationwide population-based study. *Int. J. Tuberc. Lung Dis.* **22**, 100–105 (2018).
8. Fernandez, I. E. & Eickelberg, O. Biomarkers in Interstitial Lung Diseases. in *Precision in Pulmonary, Critical Care, and Sleep Medicine: A Clinical and Research Guide* (eds. Gomez, J. L., Himes, B. E. & Kaminski, N.) 155–165 (Springer International Publishing, 2020). doi:10.1007/978-3-030-31507-8\_11.
9. Sgalla, G., Coconcelli, E., Tonelli, R. & Richeldi, L. Novel drug targets for idiopathic pulmonary fibrosis. *Expert Review of Respiratory Medicine* **10**, 393–405 (2016).
10. Hunninghake, G. M. A New Hope for Idiopathic Pulmonary Fibrosis. *N Engl J Med* **370**, 2142–2143 (2014).
11. Global, regional, and national age–sex specific all-cause and cause-specific mortality for 240 causes of death, 1990–2013: a systematic analysis for the Global Burden of Disease Study 2013. *The Lancet* **385**, 117–171 (2015).
12. Matute-Bello, G., Frevert, C. W. & Martin, T. R. Animal models of acute lung injury. *American Journal of Physiology-Lung Cellular and Molecular Physiology* **295**, L379–L399 (2008).

13. Leist, M. & Hartung, T. REPRINT: Inflammatory findings on species extrapolations: Humans are definitely no 70-kg mice. *ALTEX - Alternatives to animal experimentation* **30**, 227–230 (2013).
14. Polacheck, W. J. & Chen, C. S. Measuring cell-generated forces: a guide to the available tools. *Nature Methods* **13**, 415–423 (2016).
15. Baker, B. M. & Chen, C. S. Deconstructing the third dimension – how 3D culture microenvironments alter cellular cues. *J Cell Sci* **125**, 3015–3024 (2012).
16. Griffith, L. G. & Swartz, M. A. Capturing complex 3D tissue physiology in vitro. *Nature Reviews Molecular Cell Biology* **7**, 211–224 (2006).
17. Upadhyay, S. & Palmberg, L. Air-Liquid Interface: Relevant In Vitro Models for Investigating Air Pollutant-Induced Pulmonary Toxicity. *Toxicol Sci* **164**, 21–30 (2018).
18. Nichols, J. *et al.* Modeling the lung: Design and development of tissue engineered macro- and micro-physiologic lung models for research use. *Experimental biology and medicine (Maywood, N.J.)* **239**, (2014).
19. Freed, L. E. *et al.* Advanced Tools for Tissue Engineering: Scaffolds, Bioreactors, and Signaling. *Tissue Engineering* **12**, 3285–3305 (2006).
20. Fa-Ming Chen & Xiaohua Liu. Advancing biomaterials of human origin for tissue engineering. **53**, 86–168 (2016).
21. Santos, S. C. N. da S., Sigurjonsson, Ó. E., Custódio, C. de A. & Mano, J. F. C. da L. Blood Plasma Derivatives for Tissue Engineering and Regenerative Medicine Therapies. *Tissue Eng Part B Rev* **24**, 454–462 (2018).
22. Deus, I., Mano, J. F. & Custodio, C. Perinatal tissues and cells in tissue engineering and regenerative medicine. *Acta Biomaterialia* **110**, (2020).
23. Li, L., Scheiger, J. M. & Levkin, P. A. Design and Applications of Photoresponsive Hydrogels. *Advanced Materials* **31**, 1807333 (2019).
24. Nguyen, K. T. & West, J. L. Photopolymerizable hydrogels for tissue engineering applications. *Biomaterials* **23**, 4307–4314 (2002).
25. Lutolf, M. P. & Hubbell, J. A. Synthetic biomaterials as instructive extracellular microenvironments for morphogenesis in tissue engineering. *Nat. Biotechnol.* **23**, 47–55 (2005).

26. Tibbitt, M. W. & Anseth, K. S. Hydrogels as extracellular matrix mimics for 3D cell culture. *Biotechnology and Bioengineering* **103**, 655–663 (2009).
27. Dawson, E., Mapili, G., Erickson, K., Taqvi, S. & Roy, K. Biomaterials for stem cell differentiation. *Advanced Drug Delivery Reviews* **60**, 215–228 (2008).
28. Monteiro, C. F., Santos, S. C., Custódio, C. A. & Mano, J. F. Human Platelet Lysates-Based Hydrogels: A Novel Personalized 3D Platform for Spheroid Invasion Assessment. *Advanced Science* **7**, 1902398 (2020).
29. Custódio, C. A., Cerqueira, M. T., Marques, A. P., Reis, R. L. & Mano, J. F. Cell selective chitosan microparticles as injectable cell carriers for tissue regeneration. *Biomaterials* **43**, 23–31 (2015).
30. Annabi, N. *et al.* 25th Anniversary Article: Rational Design and Applications of Hydrogels in Regenerative Medicine. *Advanced Materials* **26**, 85–124 (2014).
31. Suki, B., Ito, S., Stamenović, D., Lutchen, K. R. & Ingenito, E. P. Biomechanics of the lung parenchyma: critical roles of collagen and mechanical forces. *Journal of Applied Physiology* **98**, 1892–1899 (2005).
32. Sugihara, H., Toda, S., Miyabara, S., Fujiyama, C. & Yonemitsu, N. Reconstruction of alveolus-like structure from alveolar type II epithelial cells in three-dimensional collagen gel matrix culture. *Am J Pathol* **142**, 783–792 (1993).
33. Derricks KE, Nugent MA, Buczek-Thomas JA, & Rich CB. Ascorbate enhances elastin synthesis in 3D tissue-engineered pulmonary fibroblasts constructs. **45**, 253–260 (2013).
34. Arora, P. D., Narani, N. & McCulloch, C. A. G. The Compliance of Collagen Gels Regulates Transforming Growth Factor- $\beta$  Induction of  $\alpha$ -Smooth Muscle Actin in Fibroblasts. *Am J Pathol* **154**, 871–882 (1999).
35. Ravichandran, R. *et al.* Functionalised type-I collagen as a hydrogel building block for bio-orthogonal tissue engineering applications. *J. Mater. Chem. B* **4**, 318–326 (2015).
36. Lotz, C. *et al.* Cross-linked Collagen Hydrogel Matrix Resisting Contraction To Facilitate Full-Thickness Skin Equivalent. *ACS Appl. Mater. Interfaces* **9**, 20417–20425 (2017).
37. Dash, B. C., Duan, K., Xing, H., Kyriakides, T. R. & Hsia, H. C. An in situ collagen-HA hydrogel system promotes survival and preserves the proangiogenic secretion of hiPSC-derived vascular smooth muscle cells. *Biotechnology and Bioengineering* 2020.06.06.137968 (2020).

38. Ajalloueiian, F. *et al.* Compressed collagen constructs with optimized mechanical properties and cell interactions for tissue engineering applications. *Int J Biol Macromol* **108**, 158–166 (2018).
39. Dunphy, S. E., Bratt, J. A. J., Akram, K. M., Forsyth, N. R. & El Haj, A. J. Hydrogels for lung tissue engineering: Biomechanical properties of thin collagen–elastin constructs. *Journal of the Mechanical Behavior of Biomedical Materials* **38**, 251–259 (2014).
40. Dunsmore SE & Rannels DE. Extracellular matrix biology in the lung. **270**, L3–L27 (1996).
41. Burgstaller, G. *et al.* The instructive extracellular matrix of the lung: basic composition and alterations in chronic lung disease. *European Respiratory Journal* **50**, (2017).
42. Benton, G., Arnaoutova, I., George, J., Kleinman, H. K. & Koblinski, J. Matrigel: from discovery and ECM mimicry to assays and models for cancer research. *Adv Drug Deliv Rev* **79–80**, 3–18 (2014).
43. Kibbey, M. C. Maintenance of the EHS sarcoma and Matrigel preparation. *Journal of Tissue Culture Methods* **16**, 227–230 (1994).
44. Wu, X., Peters-Hall, J. R., Bose, S., Peña, M. T. & Rose, M. C. Human Bronchial Epithelial Cells Differentiate to 3D Glandular Acini on Basement Membrane Matrix. *Am J Respir Cell Mol Biol* **44**, 914–921 (2011).
45. Kloxin, A. M., Kasko, A. M., Salinas, C. N. & Anseth, K. S. Photodegradable hydrogels for dynamic tuning of physical and chemical properties. *Science* **324**, 59–63 (2009).
46. Dhandayuthapani, B., Yoshida, Y., Maekawa, T. & Kumar, D. S. Polymeric Scaffolds in Tissue Engineering Application: A Review. *International Journal of Polymer Science* **2011**, 1–19 (2011).
47. Cortiella, J. *et al.* Tissue-engineered lung: an in vivo and in vitro comparison of polyglycolic acid and pluronic F-127 hydrogel/somatic lung progenitor cell constructs to support tissue growth. *Tissue Eng.* **12**, 1213–1225 (2006).
48. Mondrinos, M. J. *et al.* Engineering three-dimensional pulmonary tissue constructs. *Tissue Eng.* **12**, 717–728 (2006).
49. Uriarte, J. J., Uhl, F. E., Rolandsson Enes, S. E., Pouliot, R. A. & Weiss, D. J. Lung bioengineering: advances and challenges in lung decellularization and recellularization. *Current Opinion in Organ Transplantation* **23**, 673–678 (2018).

50. Skolasinski, S. & Panoskaltsis-Mortari, A. Decellularization of Intact Lung Tissue Through Vasculature and Airways Using Negative and Positive Pressure. in *Methods in Molecular Biology* vol. 1577 307–315 (Springer New York, 2017).
51. Obata, T. *et al.* Utilization of Natural Detergent Potassium Laurate for Decellularization in Lung Bioengineering. *Tissue Engineering Part C: Methods* **25**, 459–471 (2019).
52. Tsuchiya, T. *et al.* Ventilation-Based Decellularization System of the Lung. *BioResearch Open Access* **5**, 118–126 (2016).
53. Gilbert, T. W., Freund, J. M. & Badylak, S. F. Quantification of DNA in biologic scaffold materials. *J. Surg. Res.* **152**, 135–139 (2009).
54. Gilpin, S. E., Charest, J. M., Ren, X. & Ott, H. C. Bioengineering Lungs for Transplantation. *Thoracic Surgery Clinics* **26**, 163–171 (2016).
55. O’Neill, J. D. *et al.* Decellularization of human and porcine lung tissues for pulmonary tissue engineering. *Ann. Thorac. Surg.* **96**, 1046–1055; discussion 1055-1056 (2013).
56. Petersen, T. H., Petersen, T. H., Calle, E. A., Colehour, M. B. & Niklason, L. E. Matrix Composition and Mechanics of Decellularized Lung Scaffolds. *CTO* **195**, 222–231 (2012).
57. O’Neill, J. D. *et al.* Decellularization of Human and Porcine Lung Tissues for Pulmonary Tissue Engineering. *The Annals of Thoracic Surgery* **96**, 1046–1056 (2013).
58. Wallis, J. M. *et al.* Comparative Assessment of Detergent-Based Protocols for Mouse Lung De-Cellularization and Re-Cellularization. *Tissue Engineering Part C: Methods* **18**, 420–432 (2012).
59. Crapo, P. M., Gilbert, T. W. & Badylak, S. F. An overview of tissue and whole organ decellularization processes. *Biomaterials* **32**, 3233–3243 (2011).
60. Young, B. M. *et al.* Electrospun Decellularized Lung Matrix Scaffold for Airway Smooth Muscle Culture. *ACS Biomater. Sci. Eng.* **3**, 3480–3492 (2017).
61. Link, P. A., Pouliot, R. A., Mikhael, N. S., Young, B. M. & Heise, R. L. Tunable Hydrogels from Pulmonary Extracellular Matrix for 3D Cell Culture. *J Vis Exp.* (119):55094 (2017).
62. Pouliot, R. A. *et al.* Development and characterization of a naturally derived lung extracellular matrix hydrogel. *Journal of Biomedical Materials Research Part A* **104**, 1922–1935 (2016).

63. Petrou, C. L. *et al.* Clickable decellularized extracellular matrix as a new tool for building hybrid-hydrogels to model chronic fibrotic diseases *in vitro*. *J. Mater. Chem. B* **8**, 6814–6826 (2020).
64. Uhl, F. E., Wagner, D. E. & Weiss, D. J. Preparation of Decellularized Lung Matrices for Cell Culture and Protein Analysis. in *Fibrosis* (ed. Rittié, L.) vol. 1627 253–283 (Springer New York, 2017).
65. Crabbé, A. *et al.* Recellularization of Decellularized Lung Scaffolds Is Enhanced by Dynamic Suspension Culture. *PLoS One* **10**, (2015).
66. Booth, A. J. *et al.* Acellular Normal and Fibrotic Human Lung Matrices as a Culture System for In Vitro Investigation. *American Journal of Respiratory and Critical Care Medicine* **186**, 866 (2012).
67. Parker, M. W. *et al.* Fibrotic extracellular matrix activates a profibrotic positive feedback loop. *J Clin Invest* **124**, 1622–1635 (2014).
68. Sokocevic, D. *et al.* The effect of age and emphysematous and fibrotic injury on the recellularization of de-cellularized lungs. *Biomaterials* **34**, 3256–3269 (2013).
69. Godin, L. M. *et al.* Decreased Laminin Expression by Human Lung Epithelial Cells and Fibroblasts Cultured in Acellular Lung Scaffolds from Aged Mice. *PLoS One* **11**, (2016).
70. Jenkins, R. G. *et al.* An Official American Thoracic Society Workshop Report: Use of Animal Models for the Preclinical Assessment of Potential Therapies for Pulmonary Fibrosis. *Am J Respir Cell Mol Biol* **56**, 667–679 (2017).
71. Placke, M. E. & Fisher, G. L. Adult peripheral lung organ culture--a model for respiratory tract toxicology. *Toxicol. Appl. Pharmacol.* **90**, 284–298 (1987).
72. Liu, G. *et al.* Use of precision cut lung slices as a translational model for the study of lung biology. *Respir Res* **20**, 162 (2019).
73. Umachandran, M. & Ioannides, C. Stability of cytochromes P450 and phase II conjugation systems in precision-cut rat lung slices cultured up to 72 h. *Toxicology* **224**, 14–21 (2006).
74. Henjakovic, M. *et al.* Ex vivo testing of immune responses in precision-cut lung slices. *Toxicol. Appl. Pharmacol.* **231**, 68–76 (2008).
75. Sanderson, M. J. Exploring lung physiology in health and disease with lung slices. *Pulm Pharmacol Ther* **24**, 452–465 (2011).

76. Temann, A. *et al.* Evaluation of inflammatory and immune responses in long-term cultured human precision-cut lung slices. *Hum Vaccin Immunother* **13**, 351–358 (2017).
77. Bailey, K. E. *et al.* Embedding of Precision-Cut Lung Slices in Engineered Hydrogel Biomaterials Supports Extended *Ex Vivo* Culture. *Am J Respir Cell Mol Biol* **62**, 14–22 (2020).
78. Morin, J.-P. *et al.* Precision cut lung slices as an efficient tool for in vitro lung physiopharmacotoxicology studies. *Xenobiotica* **43**, 63–72 (2013).
79. Rosner, S. R. *et al.* Airway contractility in the precision-cut lung slice after cryopreservation. *Am. J. Respir. Cell Mol. Biol.* **50**, 876–881 (2014).
80. Li, G. *et al.* Preserving Airway Smooth Muscle Contraction in Precision-Cut Lung Slices. *Scientific Reports* **10**, 6480 (2020).
81. Lauenstein, L. *et al.* Assessment of immunotoxicity induced by chemicals in human precision-cut lung slices (PCLS). *Toxicol In Vitro* **28**, 588–599 (2014).
82. Guo, T., Lok, K. Y., Yu, C. & Li, Z. Lung Fibrosis: Drug Screening and Disease Biomarker Identification with a Lung Slice Culture Model and Subtracted cDNA Library. *Alternatives to Laboratory Animals* **42**, 235–243 (2014).
83. Uhl, F. E. *et al.* Preclinical validation and imaging of Wnt-induced repair in human 3D lung tissue cultures. *European Respiratory Journal* **46**, 1150–1166 (2015).
84. Tatler, A. L. *et al.* Caffeine inhibits TGF $\beta$  activation in epithelial cells, interrupts fibroblast responses to TGF $\beta$ , and reduces established fibrosis in ex vivo precision-cut lung slices. *Thorax* **71**, 565–567 (2016).
85. Mercer, P. F. *et al.* Exploration of a potent PI3 kinase/mTOR inhibitor as a novel anti-fibrotic agent in IPF. *Thorax* **71**, 701–711 (2016).
86. Wohlsen, A. *et al.* The early allergic response in small airways of human precision-cut lung slices. *Eur. Respir. J.* **21**, 1024–1032 (2003).
87. Johnson, J. R. *et al.* Continuous Exposure to House Dust Mite Elicits Chronic Airway Inflammation and Structural Remodeling. *Am J Respir Crit Care Med* **169**, 378–385 (2004).
88. Kumar, R. K., Herbert, C. & Foster, P. S. The ‘classical’ ovalbumin challenge model of asthma in mice. *Curr Drug Targets* **9**, 485–494 (2008).



89. Fugazzola, M., Barton, A.-K., Niedorf, F., Kietzmann, M. & Ohnesorge, B. Non-genomic action of beclomethasone dipropionate on bronchoconstriction caused by leukotriene C4 in precision cut lung slices in the horse. *BMC Vet. Res.* **8**, 160 (2012).
90. Cooper, P. R. & Panettieri, R. A. Steroids completely reverse albuterol-induced beta(2)-adrenergic receptor tolerance in human small airways. *J. Allergy Clin. Immunol.* **122**, 734–740 (2008).
91. Kasper, M. *et al.* Early signs of lung fibrosis after in vitro treatment of rat lung slices with CdCl<sub>2</sub> and TGF- $\beta$ 1. *Histochemistry and cell biology* **121**, 131–40 (2004).
92. Alsafadi, H. N. *et al.* An ex vivo model to induce early fibrosis-like changes in human precision-cut lung slices. *American Journal of Physiology-Lung Cellular and Molecular Physiology* **312**, L896–L902 (2017).
93. Lehmann, M. *et al.* Differential effects of Nintedanib and Pirfenidone on lung alveolar epithelial cell function in ex vivo murine and human lung tissue cultures of pulmonary fibrosis. *Respiratory Research* **19**, (2018).
94. Rubio, K. *et al.* Inactivation of nuclear histone deacetylases by EP300 disrupts the MiCEE complex in idiopathic pulmonary fibrosis. *Nature Communications* **10**, (2019).
95. Woodcock, H. V. *et al.* The mTORC1/4E-BP1 axis represents a critical signaling node during fibrogenesis. *Nature Communications* **10**, 6 (2019).
96. Sutherland, R. M., Inch, W. R., McCredie, J. A. & Kruuv, J. A Multi-component Radiation Survival Curve Using an *in Vitro* Tumour Model. *International Journal of Radiation Biology and Related Studies in Physics, Chemistry and Medicine* **18**, 491–495 (1970).
97. Sutherland, R. M., McCredie, J. A. & Inch, W. R. Growth of Multicell Spheroids in Tissue Culture as a Model of Nodular Carcinomas. *J Natl Cancer Inst* **46**, 113–120 (1971).
98. Hirschhaeuser, F. *et al.* Multicellular tumor spheroids: An underestimated tool is catching up again. *Journal of Biotechnology* **148**, 3–15 (2010).
99. Ekert, J. E. *et al.* Three-Dimensional Lung Tumor Microenvironment Modulates Therapeutic Compound Responsiveness In Vitro – Implication for Drug Development. *PLOS ONE* **9**, e92248 (2014).

100. Konar, D., Devarasetty, M., Yildiz, D. V., Atala, A. & Murphy, S. V. Lung-On-A-Chip Technologies for Disease Modeling and Drug Development. *Biomed Eng Comput Biol* **7**, 17–27 (2016).
101. Cui, X., Hartanto, Y. & Zhang, H. Advances in multicellular spheroids formation. *Journal of The Royal Society Interface* **14**, 20160877 (2017).
102. Costa, E. C., de Melo-Diogo, D., Moreira, A. F., Carvalho, M. P. & Correia, I. J. Spheroids Formation on Non-Adhesive Surfaces by Liquid Overlay Technique: Considerations and Practical Approaches. *Biotechnology Journal* **13**, 1700417 (2018).
103. Moshksayan, K. *et al.* Spheroids-on-a-chip: Recent advances and design considerations in microfluidic platforms for spheroid formation and culture. *Sensors and Actuators B: Chemical* **263**, 151–176 (2018).
104. Fang, Y. & Eglén, R. M. Three-Dimensional Cell Cultures in Drug Discovery and Development. *SLAS DISCOVERY: Advancing Life Sciences R&D* **22**, 456–472 (2017).
105. Klameth, L. *et al.* Small cell lung cancer: model of circulating tumor cell tumorspheres in chemoresistance. *Scientific Reports* **7**, 5337 (2017).
106. Lewis, K. J. R. *et al.* Epithelial-mesenchymal crosstalk influences cellular behavior in a 3D alveolus-fibroblast model system. *Biomaterials* **155**, 124–134 (2018).
107. Meenach, S. A. *et al.* Development of three-dimensional lung multicellular spheroids in air- and liquid-interface culture for the evaluation of anticancer therapeutics. *International Journal of Oncology* **48**, 1701–1709 (2016).
108. Zhang, Z. *et al.* Establishment of patient-derived tumor spheroids for non-small cell lung cancer. *PLoS One* **13**, e0194016 (2018).
109. Barkauskas, C. E. *et al.* Lung organoids: current uses and future promise. *Development* **144**, 986–997 (2017).
110. McCauley, K. B. *et al.* Efficient Derivation of Functional Human Airway Epithelium from Pluripotent Stem Cells via Temporal Regulation of Wnt Signaling. *Cell Stem Cell* **20**, 844-857.e6 (2017).
111. Konishi, S. *et al.* Directed Induction of Functional Multi-ciliated Cells in Proximal Airway Epithelial Spheroids from Human Pluripotent Stem Cells. *Stem Cell Reports* **6**, 18–25 (2016).

112. Miller, A. J. *et al.* In Vitro Induction and In Vivo Engraftment of Lung Bud Tip Progenitor Cells Derived from Human Pluripotent Stem Cells. *Stem Cell Reports* **10**, 101–119 (2018).
113. McQualter, J. L., Yuen, K., Williams, B. & Bertoncello, I. Evidence of an epithelial stem/progenitor cell hierarchy in the adult mouse lung. *PNAS* **107**, 1414–1419 (2010).
114. Sachs, N. *et al.* Long-term expanding human airway organoids for disease modeling. *EMBO J* **38**, (2019).
115. Miller, A. J. *et al.* Generation of lung organoids from human pluripotent stem cells in vitro. *Nature Protocols* **14**, 518–540 (2019).
116. Leibel, S. L., McVicar, R. N., Winquist, A. M., Niles, W. D. & Snyder, E. Y. Generation of Complete Multi-Cell Type Lung Organoids From Human Embryonic and Patient-Specific Induced Pluripotent Stem Cells for Infectious Disease Modeling and Therapeutics Validation. *Current Protocols in Stem Cell Biology* **54**, e118 (2020).
117. Lee, J.-H. *et al.* Lung stem cell differentiation in mice directed by endothelial cells via a BMP4-NFATc1-Thrombospondin-1 axis. *Cell* **156**, 440–455 (2014).
118. Strikoudis, A. *et al.* Modeling of Fibrotic Lung Disease Using 3D Organoids Derived from Human Pluripotent Stem Cells. *Cell Reports* **27**, 3709–3723.e5 (2019).
119. Huh, D. *et al.* Reconstituting Organ-Level Lung Functions on a Chip. *Science* **328**, 1662–1668 (2010).
120. Huh, D. *et al.* A Human Disease Model of Drug Toxicity-Induced Pulmonary Edema in a Lung-on-a-Chip Microdevice. *Science Translational Medicine* **4**, 159ra147-159ra147 (2012).
121. Blume, C. *et al.* Temporal Monitoring of Differentiated Human Airway Epithelial Cells Using Microfluidics. *PLOS ONE* **10**, e0139872 (2015).
122. Zhou, J. *et al.* Isolation of circulating tumor cells in non-small-cell-lung-cancer patients using a multi-flow microfluidic channel. *Microsystems & Nanoengineering* **5**, 1–12 (2019).
123. Ito, Y. *et al.* Lung fibroblasts accelerate wound closure in human alveolar epithelial cells through hepatocyte growth factor/c-Met signaling. *American Journal of Physiology-Lung Cellular and Molecular Physiology* **307**, L94–L105 (2014).
124. Zamprogno, P. *et al.* Second-generation lung-on-a-chip array with a stretchable biological membrane. 608919 <http://biorxiv.org/lookup/doi/10.1101/608919> (2019) doi:10.1101/608919.

125. Zhang, C., Zhao, Z., Rahim, N. A. A., Noort, D. van & Yu, H. Towards a human-on-chip: Culturing multiple cell types on a chip with compartmentalized microenvironments. *Lab on a Chip* **9**, 3185–3192 (2009).

# Chapter II

**Aims**

Fibrotic lung diseases are chronic, irreversible, age-related diseases very challenging to classify, mostly diagnosed at an advanced stage. Both animal models<sup>1,2</sup> and *in vitro* platforms<sup>3-5</sup> have been used to investigate the cellular and molecular mechanisms behind lung fibrogenesis. Animal models fail to recapitulate the human lung pathophysiology, significantly diverging from human anatomical, biological, and immunological features. In fact, the American Thoracic Society emphasized the need to develop “humanized” platforms of lung fibrotic diseases to overcome the limitations of animal models. *In vitro* models are therefore attractive tools in basic and translational studies. However, most *in vitro* studies of lung fibrosis have been performed using 2D monolayers of myofibroblasts on tissue culture plastic, which cannot accurately represent the structural three-dimensionality of native lung tissue, causing loss or changes of tissue-specific cell functions. 3D lung fibrotic models are therefore an important alternative to overcome the previously mentioned limitations. Studies using 3D cell cultures have already proven that ECM strongly influences cell behavior, in particular in fibroblasts<sup>6</sup>. Cells attach to the ECM via cell adhesion receptors, and they use them to sense the biochemical and biomechanical properties of their surrounding environment, behaving accordingly: they immediately react to the stiffness by adapting their shape and activity and are even able to frame their gene expression in the long term, as they must tune the forces they apply while contracting with the tensile strength of the ECM that holds them<sup>7</sup>. Whether ECM stiffening occurs due to exacerbated ECM molecules deposition or precedes the development of fibrosis is yet to be understood. Developing 3D lung models that enable increased rigidity of the ECM, mimicking what occurs in lung fibrogenesis is therefore of major interest. Methacryloyl platelet lysates (PLMA) hydrogels are an attractive alternative to other ECM-mimicry materials because they provide cells with both physical scaffolding and biochemical cues from human origin. The modification of PLs by chemical conjugation with a photoresponsive group allows the formation of PL-based photopolymerizable materials with tunable mechanical properties and increased stability. This material is particularly interesting to model lung fibrosis, as the mechanical stiffness of these hydrogels can be tuned to match the pathological stiffness of fibrotic human lungs by varying both the degree of methacrylation and PLMA concentration<sup>8</sup>. Therefore the main goal of this thesis was to develop a 3D model of the fibrotic lung and the specific aims were: 1) to optimize the degree of methacrylation and concentration of PLMA-based hydrogels for recapitulating the biomechanical features of the fibrotic lung, 2) to examine the cellular viability and morphology within PLMA hydrogels, and 3) to mimic the profibrotic consequences of TGF- $\beta$  stimulation in PLMA hydrogels with embedded lung fibroblasts.

## Bibliography:

1. Moore, B. B. & Hogaboam, C. M. Murine models of pulmonary fibrosis. *Am J Physiol Lung Cell Mol Physiol* **294**, L152-160 (2008).
2. B Moore, B. *et al.* Animal models of fibrotic lung disease. *Am J Respir Cell Mol Biol* **49**, 167–179 (2013).
3. Correll, K. A. *et al.* TGF beta inhibits HGF, FGF7, and FGF10 expression in normal and IPF lung fibroblasts. *Physiol Rep* **6**, e13794 (2018).
4. Hetzel, M., Bachem, M., Anders, D., Trischler, G. & Faehling, M. Different effects of growth factors on proliferation and matrix production of normal and fibrotic human lung fibroblasts. *Lung* **183**, 225–237 (2005).
5. Thannickal, V. J. *et al.* Matrix biology of idiopathic pulmonary fibrosis: a workshop report of the national heart, lung, and blood institute. *Am J Pathol* **184**, 1643–1651 (2014).
6. Liu, M., Tanswell, A. K. & Post, M. Mechanical force-induced signal transduction in lung cells. *American Journal of Physiology-Lung Cellular and Molecular Physiology* **277**, L667–L683 (1999).
7. Schiller, H. B. & Fässler, R. Mechanosensitivity and compositional dynamics of cell–matrix adhesions. *EMBO Rep* **14**, 509–519 (2013).
8. Santos, S. C., Custódio, C. A. & Mano, J. F. Photopolymerizable Platelet Lysate Hydrogels for Customizable 3D Cell Culture Platforms. *Adv Healthc Mater* **7**, e1800849 (2018).

.

# Chapter III

**Platelet lysates-based hydrogels for 3D lung modeling**



## Introduction

Interstitial lung diseases (ILD), in particular Idiopathic Pulmonary Fibrosis (IPF), are untreatable diseases associated with a median survival of 2-5 years<sup>1</sup>. These diseases have been associated with dysregulated wound healing responses, involving incessant cycles of lung tissue injury, and ECM deposition by myofibroblasts. Although there are already many identified biomolecules, mechanobiological, and cellular processes involved in lung fibrosis, current antifibrotic drugs that limit or reverse fibrosed lung remain a major clinical urgency, with organ transplantation remaining the only curative treatment option for late-stage disease. Undoubtedly, the limited efficacy of current antifibrotic drugs is in part due to the complexity of the disease, and also to the limited development of accurate biomimetic *in vitro* models for investigation of the fibrogenic remodeling of lung parenchyma. A strong correlation between lung stiffness and worst clinical outcomes suggests a critical role for matrix mechanosensing in lung fibrosis<sup>2</sup>. For many decades, research on fibroblasts interacting with 2D tissue culture plates has successfully contributed to gain insights into the mechanical activities of individual cells in response to soluble GF and/or ECM cues<sup>3,4</sup>. However, these models limit fibroblasts to the influence of one spatial plane in which cells are immobilized, forcing apical-basal polarization, limited intercellular interactions, and abnormal integrin receptor expression. Also, plastic culture plates have non-physiological stiffness (>1000 kPa), which has been reported to induce abnormal cytoskeletal organization<sup>5</sup>, disturb gene expression<sup>6</sup>, and drive epigenetic alterations of fibroblasts<sup>7</sup>. Even taking into consideration mechanical tunable substrates on which cells are studied on top of<sup>8-10</sup>, these models still cannot recapitulate the tissue-like signaling context that results when fibroblasts are completely embedded in an ECM that can be remodeled, such as in a native tissue environment. In the same line, experimental animal models have extensively contributed to elucidate the role of many ECM components in various lung conditions<sup>11-13</sup>. However, these models fail to mimic human diseases, raising difficulties in translating animal results to human applications.

On the contrary, 3D matrices allow lung fibroblasts to adhere to their substrate at many focal adhesion points, and to experience more physiological stress-strain and soluble gradients. Although there are already studies of lung cells cultured within 3D matrices<sup>14</sup>, few studies have investigated the viability, morphology, and behavior of lung fibroblasts within a stiff matrix.

## Cellular and biochemical mechanisms in fibrosis

Fibroblasts are tissue mesenchymal cells that contribute to tissue function and architecture by producing ECM's structural proteins (such as collagens and elastin), adhesive proteins (e.g. laminin and fibronectin), and ground substance (glycosaminoglycans)<sup>15</sup>. Upon injury, epithelial cell activation and epithelial-mesenchymal signaling trigger fibroblast activation and recruitment to the wound site, where they produce ECM proteins to build a provisional matrix for tissue regeneration.

Fibroblasts have been implicated in several clinical conditions related to abnormalities in wound healing; for example, fibroblasts isolated from fibrotic lung tissue have an increased ability to produce ECM proteins, exhibit enhanced resistance to apoptosis, produce ROS, secrete less antifibrotic factors, and have increased invasion abilities, therefore exerting a profibrotic effect<sup>16-21</sup>. Fibroblasts are also one of the precursor cells for myofibroblast differentiation. Myofibroblasts express characteristics of both smooth muscle cells and fibroblasts, as they exhibit packs of stress fibers, focal adhesion complexes, and express  $\alpha$ -SMA<sup>22</sup>. These cells are believed to be key effectors in tissue scarring<sup>23,24</sup>; under normal wound healing circumstances, myofibroblasts undergo apoptosis or revert to inactive phenotype once the provisional scar tissue is degraded and tissue healing is accomplished. However, in fibrotic diseases, myofibroblasts persist in their activated state. Excessive myofibroblast activity, including overproduction of ECM components and excessive wound contraction, are major contributors to the formation of scar tissue<sup>25</sup> and are essentially promoted by TGF- $\beta$ 1 and by mechanical signals<sup>22</sup>. TGF- $\beta$  is one of the most studied cytokines, and is implicated in several cellular functions, including tissue homeostasis regulation, wound repair, immunity and inflammation, ECM deposition, and cell differentiation, proliferation, and apoptosis<sup>26,27</sup>. Of the three structurally similar isoforms that have been identified in mammals (TGF- $\beta$ 1, 2, and 3), TGF- $\beta$ 1 is prevalent<sup>26</sup>, and it is produced by many cell types in the ECM as a latent complex waiting to be activated. In its inactive state, TGF- $\beta$  is bound to a latency-associated peptide (LAP), preventing it to bind to TGF- $\beta$  receptors<sup>26</sup>. TGF- $\beta$  activation requires disruption of the TGF- $\beta$ -LAP complex, and this process usually involves conformational changes in LAP, which can be induced by ROS<sup>28</sup>, contractile forces transmitted by integrins<sup>29</sup>, proteolytic cleavage (by plasmin, MMP2, MMP9)<sup>30,31</sup>, or pH changes<sup>32</sup>. Once in its active form, TGF- $\beta$  can induce signaling by binding to transmembrane type I (T $\beta$ RI) and type II receptors (T $\beta$ RII), which are serine/threonine kinases. Once TGF- $\beta$  binds to T $\beta$ RII, T $\beta$ RI is recruited into the complex where it is phosphorylated and activated by T $\beta$ RII, forming a stable heteromeric complex.

TGF- $\beta$ 1 plays a pivotal role in the pathogenesis of lung fibrosis, participating in fibroblasts recruitment and activation into myofibroblasts<sup>33</sup>, inhibiting fibroblast apoptosis<sup>34</sup>, inducing epithelial-mesenchymal transition (EMT)<sup>35</sup>, AEC apoptosis<sup>36</sup>, and ECM synthesis and deposition<sup>37</sup>. Considering their central role in fibrosis, investigating lung fibroblasts and TGF- $\beta$  signaling could help us identify new fibrotic pathways and mediators and therefore improve the clinical approaches used to treat lung fibrotic diseases.

## **Platelet-based biomaterials as humanized 3D models**

Platelets are known to have a pivotal role in preventing blood loss at sites of vascular injury<sup>38</sup>. They adhere to the ruptured endothelium and form a procoagulant surface that enhances thrombin generation and the formation of a dense fibrin network. However, besides their thrombotic role, they also contribute to several other mechanisms in tissue renewal and wound healing<sup>39</sup>, being critically involved in angiogenesis, renovation of connective tissue, and restoration of tissue-specific cell types<sup>40</sup>. They contain secretable granules (mainly alpha[ $\alpha$ ]-granules) that store multiple proteins, cytokines, and GFs that are released upon platelet activation. These substances are able to bind to a developing fibrin network or components of the ECM (collagen, glycosaminoglycan, adhesive proteins), establishing chemotactic gradients that favor cell recruitment, migration, and differentiation, therefore promoting tissue regeneration<sup>38</sup>. Additionally, platelets contribute to the defense against pathogens, as they recruit immune cells, and release microbicidal molecules, including reactive oxygen species (ROS), kinocidins (e.g. platelet factor 4), defensins (e.g.  $\beta$ -defensin 2), thrombocidines (e.g. neutrophil-activating peptide-2 and connective tissue-activating peptide-III) and proteases<sup>38,41</sup>. The blood coagulation cascade and crosstalk with platelets that ultimately leads to wound healing and tissue regeneration builds up the rationale for the use of platelet-derived preparations for biomaterial applications.

The use of platelet-derived products started 40 years ago with the use of fibrin glues to seal wounds and accelerate tissue healing<sup>38</sup>. *In vivo*, besides its role in hemostasis, fibrin constructs also contribute as a scaffold for tissue regeneration as they display a microporous structure and ligands by which cells and cell mediators attach on, therefore allowing for cell adhesion, spreading, migration and proliferation<sup>42</sup>. In addition to their bioactivity, these natural-forming gels are biodegradable because they can be gradually degraded by cell-derived proteases, such as plasmin and matrix metalloproteinases (MMPs), therefore easily achieving host integration<sup>43</sup>. Fibrin hydrogels are prepared from commercially purified fibrinogen and purified thrombin<sup>43</sup>. Fibrin

hydrogels have been used as a suitable scaffold for cardiac<sup>44-48</sup>, adipose<sup>49</sup>, ocular<sup>50-52</sup>, muscle<sup>53</sup>, liver<sup>54</sup>, skin<sup>55</sup>, cartilage<sup>56</sup>, and bone TE<sup>57</sup>. However, fibrin has low mechanical properties and even the action of cultured cells tends to shrink the hydrogels, and proteolytic degradability is accelerated during *in vitro* cell culture<sup>58</sup>. Considering its softness, fibrin is often combined with other materials, such as polyurethane, polycaprolactone-based polyurethane polycaprolactone,  $\beta$ -tricalciumphosphate,  $\beta$ -tricalciumphosphate/polycaprolactone, and PEG, in order to improve its mechanical properties<sup>58</sup>. Also, different strategies have been established to overcome premature shrinking and degradability of fibrin hydrogels, such as alterations in fibrinogen and thrombin concentrations, and the addition of degradation inhibitors and crosslinking factors<sup>59</sup>. Besides fibrin, other preparations have been developed through the activation of platelet-based concentrates, contributing nowadays as helper tools in several medical and surgical procedures<sup>60,61</sup>. Platelet derivatives, including platelet-rich plasma (PRP), fibrin glue (FG), platelet gel (PG), plasma rich in growth factors (PRGF), and platelet lysates (PL), can be obtained from autologous or allogenic sources. The first have the advantage of avoiding immune reactions related to allogenic proteins. However, platelet count and GF richness of autologous platelet derivatives are inherently dependent of the patients' biological conditions<sup>62</sup>. Allogenic sources, on the other hand, are prepared from healthy donor blood following specific working procedures that assure the quality and safety of the final product<sup>63,64</sup>. PRP can be used directly as a liquid formulation or activated by the addition of calcium salts, thrombin, thromboplastin, or collagen, which leads to the formation of a fibrin network rich in activated platelets (PG)<sup>65</sup>. The degranulation of activated platelets gives rise to a plasma solution rich in GFs and cytokines, called PRGF. PRP can be also used to prepare PL through platelet lysis via freezing-thawing cycles or ultrasounds, which disrupt platelets'  $\alpha$ -granules, therefore releasing their content<sup>66</sup>.

PL are a US Food and Drug Administration-approved medium supplement for cell culture. In fact, many studies have already reported the superior effects of PL supplementation for supporting cell proliferation, differentiation, and tissue regeneration compared to FBS and PRP<sup>67</sup>. PL have also been used to form hydrogels, again by adding a clot activator. Unlike fibrin-only hydrogels, PL hydrogels contain several structural proteins other than fibrinogen. Extracellular proteins (i.e. fibronectin and collagen), proteoglycans, and adhesion proteins reinforce the fibrin network, favoring GF release kinetics. Pioneer studies demonstrated the possibility of expanding mesenchymal stromal cells (MSCs) using PL-based gels<sup>68,69</sup>. Also, MSCs were encapsulated in a 3D PL-based scaffold, and these matrices induced MSCs chondrogenic differentiation, ECM production, and isogenous group formation, suggesting their ability to support cartilage regeneration<sup>70</sup>. A work from Robinson *et al.*

also showed the ability of PL hydrogels to exert proangiogenic effects, supporting the formation of capillary networks<sup>71</sup>. Similarly, the potential of PL hydrogels to amplify and differentiate endothelial colony-forming cells into endothelial capillary networks was assessed<sup>72</sup>. The authors confirmed that angiogenic GFs present in PL created a chemotactic, mitogenic gradient that induced endothelial and perivascular cells to proliferate, therefore forming an extensive capillary network<sup>72</sup>. Altogether, this evidence suggests that PL gels hold great promise in enhancing cell expansion and invasion, and in promoting vascular regeneration. However, similarly to fibrin-only gels, they have weak mechanical properties and low stability *in vitro*, tending to degrade fast when no antifibrinolytic agent is added<sup>69</sup>, thus failing to provide a temporary scaffold system required for tissue regeneration. Considering this, PRP and PL have been combined with other biopolymers. So far, several hybrid biomaterials with enhanced mechanical properties have been developed by either incubating PL solution with the polymeric matrix, or by mixing PL with the polymeric precursor before hardening<sup>73</sup>. Also, considering that most natural polymers do not crosslink in a stable structure at physiological temperatures, chemical crosslinking can be applied. Among various crosslinking strategies, photocrosslinking has been widely used for the preparation of hydrogels for TE<sup>74</sup>. Photocrosslinking relies on the use of a photoinitiator, which promotes crosslinking upon exposure to specific wavelengths. The functionalization of natural and synthetic polymers with reactive groups such as acrylates, fumarates, or vinyl esters, is also indispensable for the photopolymerization. Our research group recently developed an advanced 3D *in vitro* platform made of PL derived photopolymerized hydrogels<sup>69</sup>. The modification of PL structural proteins with methacrylic anhydride (MA), a photoresponsive group, led to the formation of PL-based photopolymerizable materials with tunable mechanical properties. Their biochemical richness and allogeneic character, along with the ability to control shape, size, and stiffness of PLMA-hydrogels makes them superior cell culture platforms for tissue modeling.

## **PLMA-based hydrogels to model the fibrotic lung**

PLMA hydrogels are particularly interesting to model lung fibrosis, as the mechanical stiffness of these hydrogels can be tuned to match the pathological stiffness of fibrotic human lungs, which may be useful for the study of cell behavior and phenotypic changes that are intrinsically related to profibrotic matrix cues. By varying both degree of methacrylation and/or PLMA concentration, we can obtain totally different hydrogels for several biomimicry applications, including load-bearing soft tissues like the lung, with enhanced mechanical properties and stability. Furthermore, this

material platform allows matrix stiffening in the presence of cells, recapitulating the dynamic nature of what happens *in vivo* in many biological processes, such as tissue repair. Also, matrix stiffening occurs in a well-controlled manner, allowing us to create structural homogeneous and stable hydrogels<sup>69</sup>. Moreover, PLMA are of human origin, providing the cultured cells with allogeneic biochemical cues, being able to support cell adhesion and proliferation.

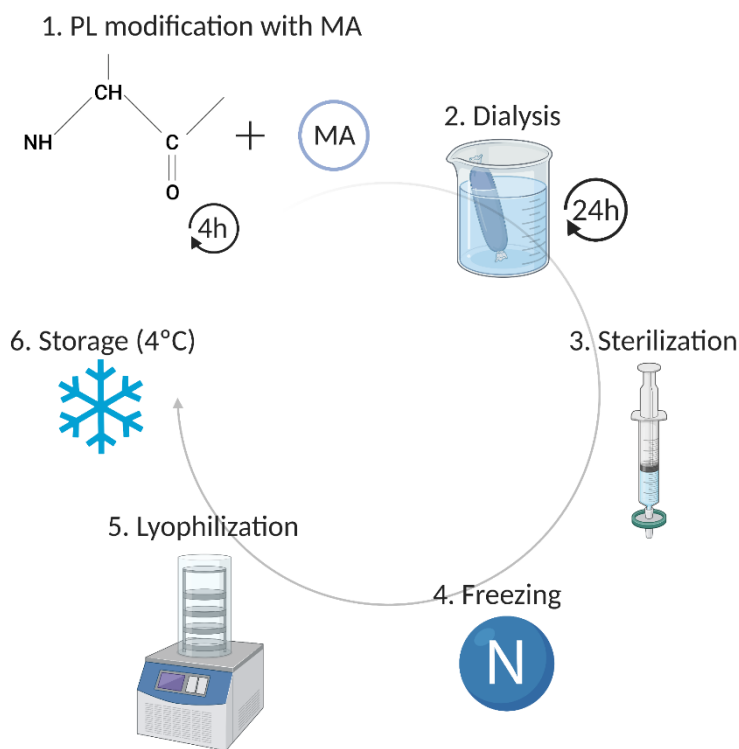
In this work, our goal was to develop a humanized 3D model that mimic pathological lungs, and thus, with an elastic modulus similar to the fibrotic lungs (15-100 kPa<sup>75</sup>). So, two degrees of methacrylation (PLMA100 and PLMA200) were tested for fibroblast culture. In the PLMA with a low degree of modification (PLMA100), cells remained viable for 7 days in culture and acquired their typical spindle-like shape, contrary to fibroblasts cultured in PLMA with a higher degree of methacrylation (PLMA200), which exhibited minimal interaction with these matrices and acquired a round morphology. Furthermore, fibroblasts cultured on PLMA100 hydrogels were able to induce marked matrix deformations right the day after encapsulation, demonstrating the feasibility of these hydrogels to induce ECM remodeling by fibroblasts, similarly to fibrotic conditions. Lastly, stimulation of photoencapsulated fibroblasts with TGF- $\beta$  resulted in no differences in Young's moduli of PLMA100 hydrogels. This model may provide the means to investigate the complex interactions between cells and their surrounding microenvironment that occur in fibrotic lung diseases, as well as the behavior and phenotypic changes in cells induced by mechanical interactions and biochemical signals and could also contribute to the development of physiologically relevant preclinical drug screening platforms.

## Experimental Section

### Synthesis of Methacryloyl Platelet Lysates (PLMA)

PLMA were synthesized following a procedure that was previously reported by our research group (**Figure 4**)<sup>69</sup>. Shortly, PL (STEMCELL Technologies, Canada) were thawed in a water bath at 37°C. Then, PLMA of low-degree modification (PLMA100) and high-degree of modification (PLMA200) were synthesized by reaction with MA 94% (Sigma-Aldrich, USA) in a ratio of 100:1 (v/v) and 200:1 (v/v), respectively. The reaction was performed for 4h at room temperature, under constant stirring, and pH was maintained between 6-8 using sodium hydroxide (NaOH, 5 M) (AkzoNobel, USA) solution. Synthesized PLMA100 and PLMA200 were then purified by dialysis using SnakeSkin Dialysis Tubing (Thermo Fisher Scientific – US) against deionized water for 24h, to remove the

excess of MA. The PLMA100 and PLMA200 solutions were sterilized with a 0.2 $\mu$ m filter (Enzymatic S. A., Portugal), frozen with liquid nitrogen, lyophilized (LyoQuest Plus Eco, Telstar, Spain), and stored at 4 °C until further use.



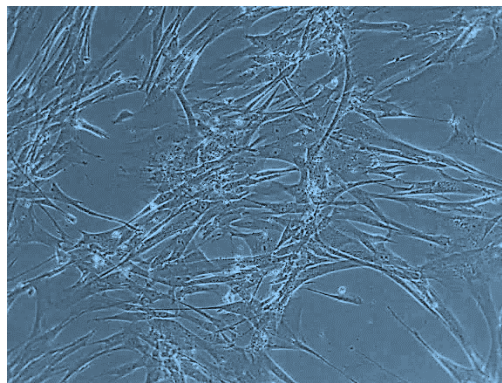
**Figure 4.** Illustrative representation of PLMA preparation.

### Preparation of PLMA hydrogels

PLMA hydrogels were prepared following a previously reported protocol<sup>69</sup>. Shortly, a 0.5% (w/v) solution of the photoinitiator 2-hydroxy-4'-(2-hydroxyethoxy)-2-methylpropiophenone (Sigma-Aldrich, Germany), also known as Irgacure, was prepared in phosphate buffered saline (PBS) (Sigma-Aldrich, USA), and then syringe filtered for sterilization. To prepare PLMA solutions, the needed amount of lyophilized PLMA were weighed and dissolved in the filtered Irgacure solution to a final concentration of 10%, 15%, and 20% w/v. The PLMA solutions were then placed in molds and irradiated with light for photopolymerization.

## Cells culture experiments

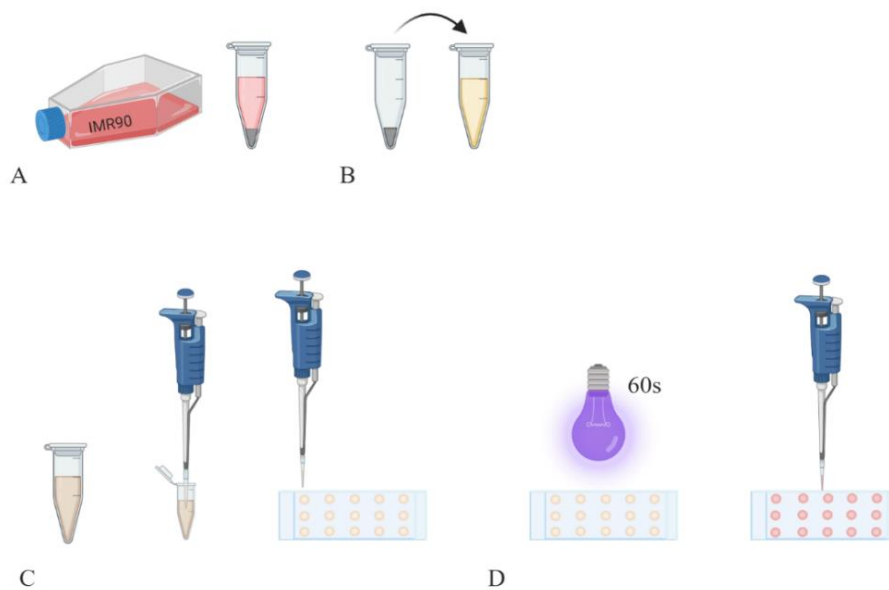
IMR90 cells (European Collection of Authenticated Cell Cultures), which are human lung fibroblasts, were cultivated in growth medium, which consisted of RPMI1640 (Thermo Fisher Scientific, USA) supplemented with Sodium Bicarbonate ( $2.4\text{g L}^{-1}$ ) (Sigma-Aldrich, USA), HEPES ( $2.4\text{g L}^{-1}$ ), 1% Sodium Pyruvate, 10% heat-inactivated fetal bovine serum (FBS) (Thermo Fisher Scientific, USA), and 1% antibiotic/antimycotic (Thermo Fisher Scientific, USA) (**Figure 5**). Cells were cultured in an incubator at  $37\text{ }^{\circ}\text{C}$  with 5%  $\text{CO}_2$  and 95% air in complete humidity (standard culture conditions) and passaged at about 80% confluence. The medium was replaced every two days.



**Figure 5.** IMR90 cell line at passage 7.

For the encapsulation experiments, cell suspensions were prepared. Cells cultured in T175 flasks were enzymatically lifted by trypsinization (0.25% (w/v) trypsin/EDTA solution, Sigma-Aldrich, Germany) after reaching 80% of confluence. After trypsin inactivation with growth medium, the cell suspension was washed with growth medium by centrifuging twice in media. Cells were resuspended to a final density of  $5.0 \times 10^6$  cells/mL in PLMA solution. Then,  $10\mu\text{l}$  of the cell suspension was pipetted into the  $\mu$ -Slide plates (ibidi, Germany) and hydrogels were reticulated by exposing them to UV radiation ( $0.95\text{ W/cm}^2$ ) during 60s (**Figure 6**). Encapsulated cells were incubated for up to 7 days, under the same cell culture conditions described above, with medium being changed every two days.





**Figure 6.** Illustrative representation of IMR90 encapsulation within PLMA100 hydrogels. A: cell count and centrifugation. B: Resuspension of cell pellet in PLMA100 solution. C: PLMA100 cell suspension pipetting into the plate. D: Photopolymerization of PLMA100 hydrogels with UV light for 60s and addition of growth medium.

## Biological performance of PLMA-based hydrogels

### Cell viability: LIVE/DEAD Assay

A LIVE/DEAD cell assay (Thermo Fisher Scientific, USA), which is a staining method that distinguishes viable from non-viable cells, was performed at 1, 3, and 7 days post-encapsulation, following the manufacturer's instructions. Briefly, the hydrogels were incubated in a solution of 1:100 of Calcein AM solution in PBS, to stain viable cells in green, and 1:200 of propidium iodide (PI), to stain non-viable cells in red, in PBS at standard culture conditions (5% CO<sub>2</sub> at 37 °C) for 30min. After washing with PBS, cell viability was observed under a fluorescence microscope (Fluorescence Microscope Zeiss, Axio Imager 2, Carl Zeiss, Germany).

### Cells morphology: Immunostaining

To access cell morphology in PLMA100 hydrogels, a DAPI/Phalloidin staining was performed. At 7 days post-encapsulation, hydrogels were washed with PBS and fixed with a 4% formaldehyde (Sigma-Aldrich) solution for at least 1 hour. For DAPI/Phalloidin staining, a phalloidin solution (Flash Phalloidin™ Red 594, 300U, Biolegend, USA) was diluted 1:40 in PBS and hydrogels were incubated at room temperature in phalloidin solution for 45 min. After washing with PBS, a DAPI (4',6-diamidino-2-phenylindole, 44 dihydrochloride), Thermo Fisher Scientific) solution was diluted at

1:1000 in PBS and hydrogels were incubated for 5 minutes with this solution at room temperature. DAPI binds to DNA, staining in blue the nucleus, and phalloidin binds to the cytoskeleton filaments, showing them in red at the fluorescence microscope. After washes with PBS, hydrogels were examined using a fluorescence microscope (Fluorescence Microscope Zeiss, Axio Imager 2, Zeiss, Germany).

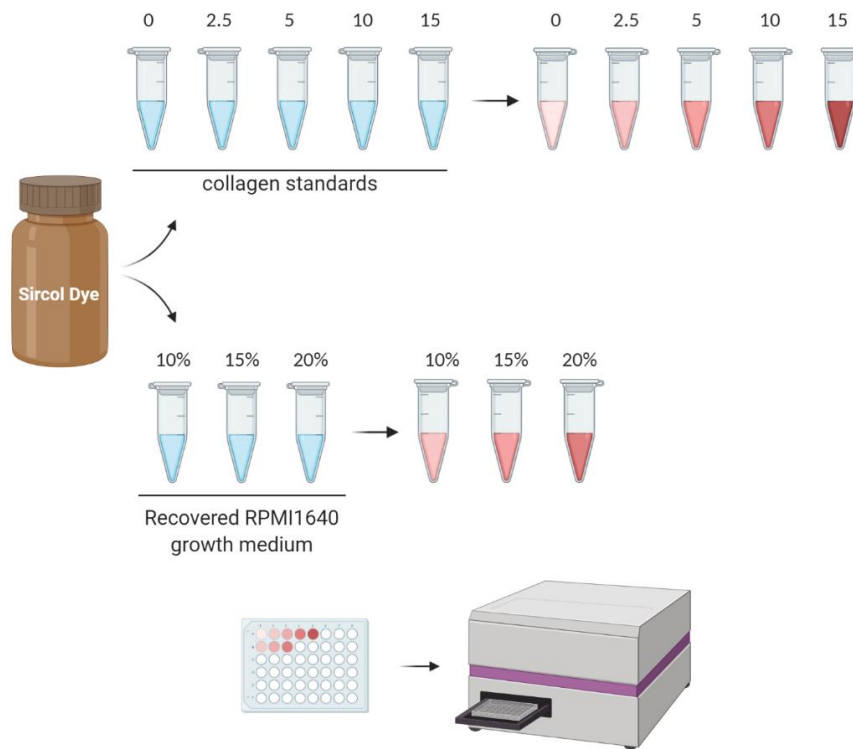
## **Compressive Mechanical Testing**

The mechanical behavior of both PLMA100 and PLMA200 hydrogels at 10%, 15%, and 20% w/v was evaluated by compression testing using the Instron 3340 Series Universal Testing System (Instron, USA), at room temperature. Young's modulus, which is indicative of gel's resistance to deformation, was defined as the slope of the linear region (0–5% of strain) of the strain–stress curve. Ultimate stress and ultimate strain values were taken as the point where failure of the hydrogel occurred.

To evaluate the effects of both TGF- $\beta$  stimulation and stiffness-dependent mechanical remodeling of PLMA100 hydrogels, IMR90 cells were incubated for 3 days in growth medium, supplemented with ascorbic acid (AA) (50 $\mu$ g/mL), as AA increases the secretion of mature collagens, and TGF- $\beta$  (2ng/mL). PLMA100 hydrogels without cells were also prepared as a control and incubated for 3 days under the same culture conditions as for PLMA100 hydrogels with encapsulated cells. The mechanical behavior of PLMA100 hydrogels was further characterized by compression testing using the Instron 3340 Series Universal Testing System (Instron, USA), at room temperature. The diameter of all hydrogels was 6mm.

## **Sircol™ Soluble Collagen Assay**

The Sircol™ Collagen Assay (Biocolor assays) is a quantitative colorimetric assay based on Sirius red for measurement of both acid-soluble and pepsin-soluble collagens. IMR90 fibroblasts were encapsulated in PLMA100 hydrogels at 10%, 15%, and 20% w/v to a final cellular density of 5.0x10<sup>6</sup> cells/mL of PLMA solution, and incubated for 48h in growth medium supplemented with AA (50 $\mu$ g/mL), and stimulated with TGF- $\beta$  (2ng/mL). After 48h, cell culture medium was recovered from the plate and collagens released into the medium were measured using a Sircol Soluble Collagen Assay kit (Biocolor assays) according to the manufacturer's instruction (**Figure 7**). PLMA100 hydrogels without embedded cells were used as negative controls.



**Figure 7.** Illustrative representation of collagen quantification using Sircol Assay Kit. A: Standards (values expressed in  $\mu\text{g}$ ) and sample preparation; B: Microplate reading at 555nm.

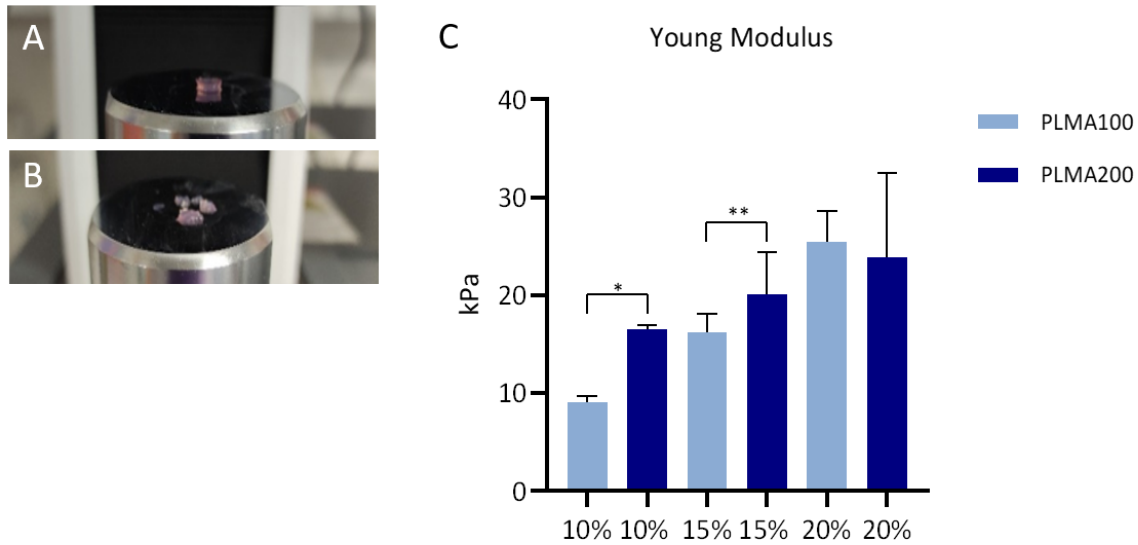
## Statistical analysis

All data were subjected to statistical analysis using GraphPad Prism 8 and were reported as a mean  $\pm$  standard deviation. Statistical differences between the analyzed groups were determined by unpaired *t*-test.

## Results and Discussion

Fibroblasts play key roles in synthesizing, organizing, and maintaining connective tissues during homeostasis and in response to injury and fibrotic disease. Their ability to exert their functions depends on their ability to sense and apply mechanical forces and to remodel the ECM<sup>76,77</sup>. In order to optimize the conditions to obtain PLMA hydrogels with an elastic modulus between 15 and 100 kPa, similarly to what is found in the fibrotic lung, we prepared hydrogels with different degrees of methacrylation (low degree: PLMA100, and high degree: PLMA200), and concentrations (10%, 15%, and 20% w/v). The mechanical behavior of PLMA hydrogels was characterized by mechanical

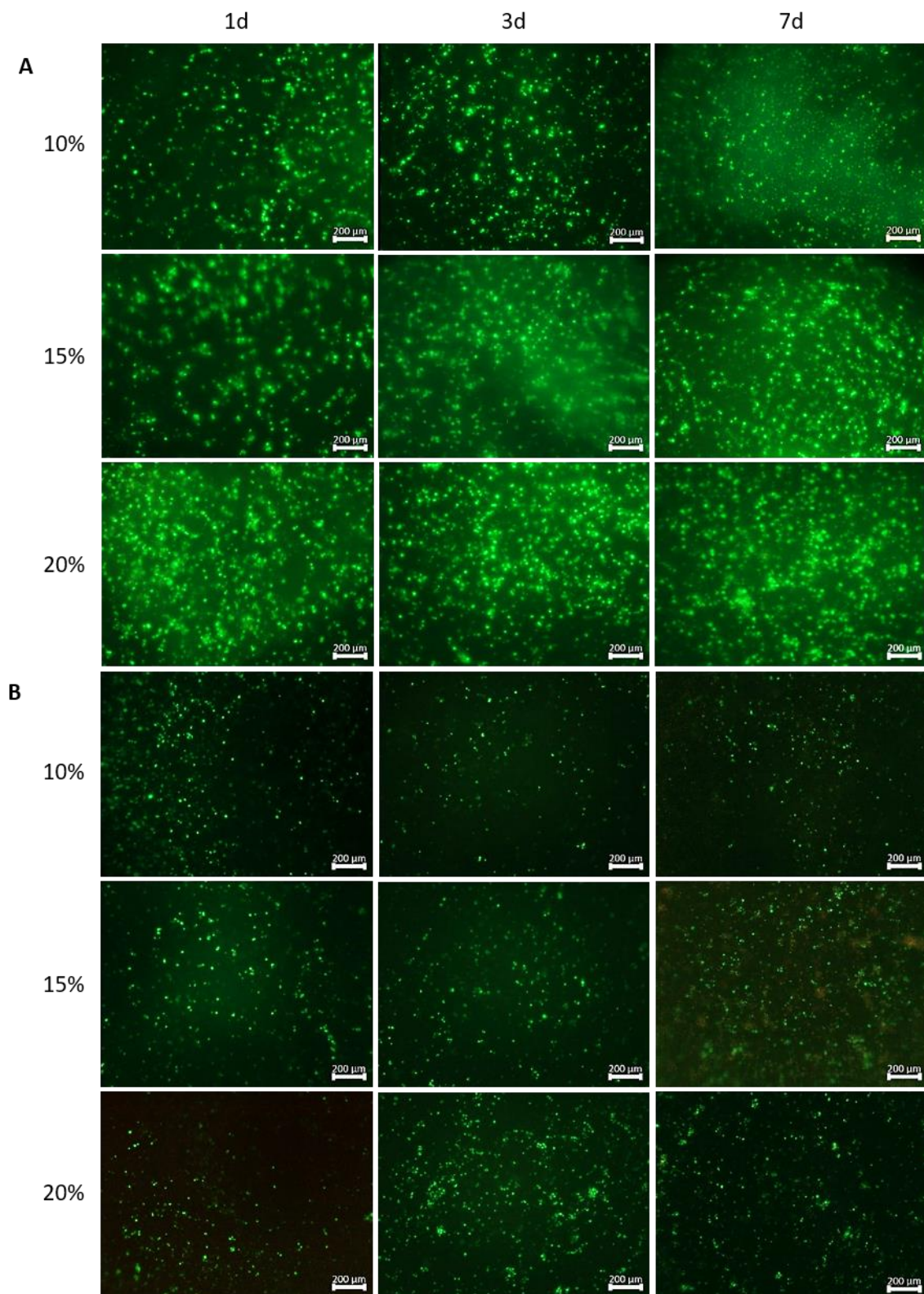
compression (**Figure 8A, 8B**) and it was found that both PLMA100 and PLMA200 hydrogels meet the pathological stiffness of fibrotic lungs. Also, PL methacrylation increased hydrogel stiffness in a concentration-dependent manner, and higher degrees of methacrylation resulted in stiffer hydrogels, therefore following the pattern already reported (**Figure 8C**)<sup>69</sup>.



**Figure 8.** PLMA hydrogels before (**A**) and after (**B**) mechanical compression, and Young Modulus of PLMA100 and PLMA200 hydrogels at 10%, 15%, and 20% w/v (**C**). Statistical analysis through unpaired *t*-test showed significant differences (\* $p < 0.05$ ) between the analyzed groups ( $n=3$ ).

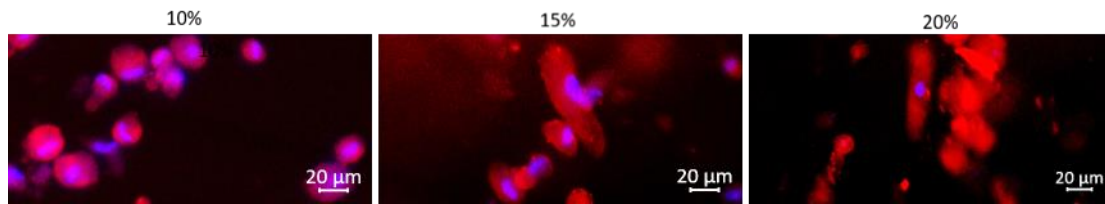
The mechanical features of hydrogels affect cell behavior and should be considered when engineering a specific tissue. Evidence shows that many cellular processes, including cell adhesion and proliferation, are strongly correlated with matrix stiffness, as it affects the formation of nutrients, oxygen, and waste products gradients, and also influences the availability of binding sites for cells to attach. To analyze the viability of lung fibroblasts in the different PLMA hydrogels, IMR90 cells were encapsulated in the biomaterials, before LIVE/DEAD staining. As observed by fluorescence microscopy, cells were alive and evenly distributed within all three PLMA100 concentrations (**Figure 9A**). To better observe cellular morphology, actin was stained with phalloidin at day 7 of incubation. Fluorescence imaging suggests that cells adhered to the matrix, with cells cultured in PLMA100 hydrogels at 15% and 20% w/v adopting a spindle-like shape (**Figure 10**). In PLMA100 at 10% w/v encapsulated fibroblasts remained viable but did not exhibit extensions, neither were organized in parallel strips as cells cultured on both PLMA100 at 15% and 20% w/v hydrogels (**Figure 10**), which is a typical pattern observed in 3D fibroblastic foci *in vivo*<sup>78,79</sup>. On the contrary, LIVE/DEAD staining revealed that cells in PLMA200 hydrogels had reduced viability when compared with PLMA100-cultured cells (**Figure 9B**). Surviving cells exhibited minimal

interaction with the matrix in all three PLMA200 concentrations (10%, 15%, and 20% w/v), and retained a round morphology at all three time points (1, 3, and 7 days) (**Figure 9B**). These contrasting results might be related to matrix porosity and pore size. It is well known that controlling the pore size and porosity of the 3D scaffolding material directly governs cell survival and proliferation to create a functional hydrogel and secrete ECM<sup>80–84</sup>. Although we did not investigate these parameters in neither PLMA100 nor PLMA200 hydrogels, scaffold porosity decreases with stiffness increases<sup>85</sup>, so the pore size of PLMA hydrogels decreases with increases in the modification degree of PL, and also with increases in protein concentration. This could explain why cells reacted better to less modified substrates (PLMA100 hydrogels). In fact, optimal fibroblast proliferation in 3D scaffolds is achieved with a pore size of 200–250 $\mu\text{m}$  and a porosity of about 86%<sup>86</sup>. Although PLMA100 hydrogels are not in this range of pore size (15–60 $\mu\text{m}$ <sup>69</sup>), cells did survive but a slight decrease in pore size in PLMA200 compared to PLMA100 may still compromise fibroblasts viability, as cell migration and nutrient and oxygen diffusion could be limited. Another possibility is that residual MA byproducts and unreacted MA that may have remained on the methacrylated PL and in the photocrosslinked PL hydrogels, which are potentially cytotoxic, could have adversely affected the viability of encapsulated cells<sup>87</sup>.



**Figure 9.** Representative fluorescence images for IMR90 upon LIVE/DEAD staining at 1, 3, and 7 days of culture in **(A)** PLMA100 and **(B)** PLMA200 hydrogels at 10%, 15%, and 20% w/v. Images are representative of 8 independent experiments.

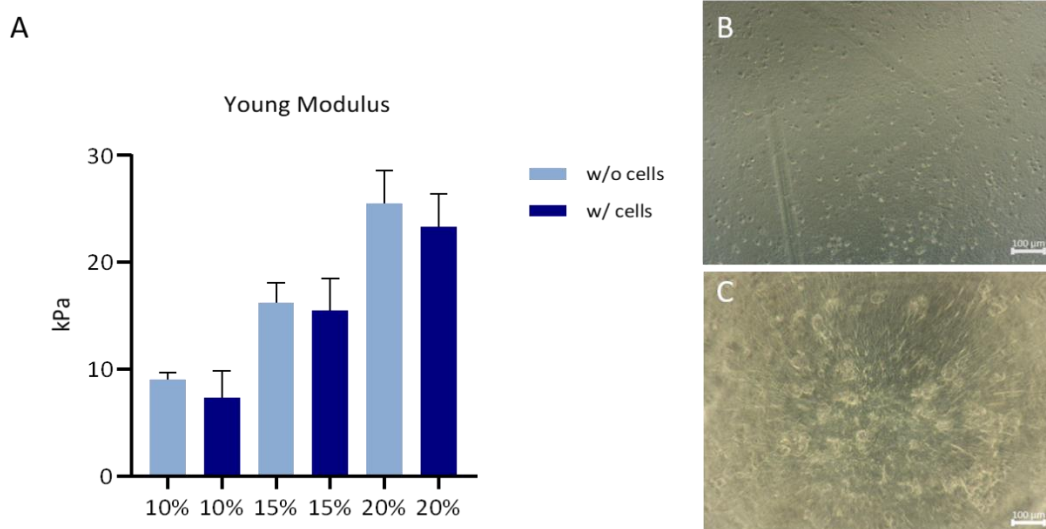




**Figure 10.** Representative fluorescence images for DAPI (blue) and phalloidin (red) staining to label the nuclei and actin cytoskeleton of IMR90 cells at 7 days of culture in PLMA100 10%, 15%, and 20% hydrogels. Images are representative of 2 independent experiments.

Considering that PLMA200 hydrogels did not support IMR90 viability, we focused on PLMA100 as a potential candidate for 3D lung modeling of fibrosis.

During fibroblast-induced matrix remodeling, mechanical cues from the remodeled ECM feedback to modulate fibroblast behavior in a reciprocal process. We thus analyzed the effect of stimulating matrix production with TGF- $\beta$  on the hydrogel mechanical properties. We found that TGF- $\beta$  stimulation of PLMA-encapsulated cells did not result in mechanical alterations in PLMA100 hydrogels, as no differences were observed in Young's moduli for PLMA100 with and without cells in neither PLMA100 concentrations (**Figure 11A**). However, we were able to macroscopically observe prominent substrate deformations the day after IMR90 encapsulation (**Figure 11B, 11C**), suggesting that even though lung fibroblasts participate in matrix rearrangements within PLMA100 hydrogels, 3 days of profibrotic stimulation with TGF- $\beta$  was probably not enough time to induce ECM deposition to the point of causing measurable changes in Young's modulus of PLMA100 hydrogels.

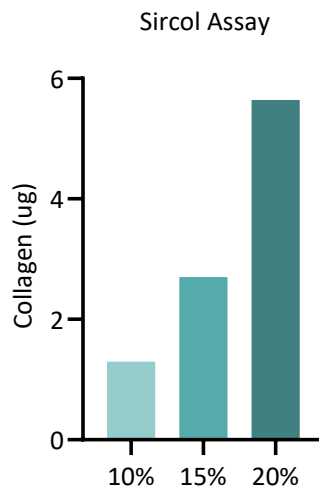


**Figure 11.** Young Modulus of PLMA100 hydrogels at 10%, 15%, and 20% w/v after 3d of TGF- $\beta$  stimulation (**A**), and representative images of IMR90 fibroblasts encapsulated in PLMA100 hydrogels at day 0 (**B**) and 1 (**C**) day of culture. Statistical analysis through unpaired *t*-test showed no significant differences ( $*P < 0.05$ ) between the analyzed groups ( $n=2$ ).

Analyzing the Young modulus of PLMA100 hydrogels and comparing these results with the analysis of the viability and morphology of IMR90 cells in these scaffolds, we can see that, although viable in PLMA100 at 10% w/v, cells preferred stiffer substrates to form stable focal adhesions: as observed by fluorescence microscope, they responded better to the PLMA hydrogels at 15%, and 20% w/v, which are stiffer than PLMA hydrogels at 10% w/v. These observations are in agreement with previous studies, showing that fibroblasts are highly sensitive to the stiffness of the substrates in both 2D and 3D matrices<sup>88</sup>. Besides experiencing an elastic modulus of  $\sim 1$  kPa *in vivo*<sup>89</sup>, human lung fibroblasts are able to adhere and proliferate on hard, stiff matrices *in vitro*<sup>10,90</sup>, better than in softer matrices where they usually exhibit low contractile forces as well as reduced spreading and replication<sup>10,91</sup>.

Besides mechanical testing, we also evaluated the collagen synthesis by fibroblasts encapsulated in PLMA100 hydrogels after stimulation with TGF- $\beta$  for 48h using a Sircol Assay on recovered growth medium. Our results show that increasing PLMA100 concentration resulted in higher amounts of collagen released to the growth medium (**Figure 12**). However, the quantification of net secretion of collagen should carefully considered, because we faced some issues when using Sircol Soluble Collagen Assay kit. Sircol dye reagent contains Sirius Red in picric acid, which has been formulated to bind specifically to collagen. However, despite not having collagen in their composition, absorbance readings at 555nm for the growth medium recovered from control PLMA hydrogels without cells showed some inespecific binding. Thus, to each sample we subtracted the absorbance of the respective negative control and our preliminary results were in agreement with previous studies. As already discussed, higher concentrations of PLMA100 result in stiffer hydrogels, which means that increasing matrix stiffness had a stimulatory effect on lung fibroblasts, inducing collagen synthesis in PLMA100 hydrogels. Matrix stiffness has already been proven to have critical implications on cultured lung fibroblasts, which exhibit mechanotransduction<sup>92,93</sup>, and have “mechanical memory”<sup>8</sup>.





**Figure 12.** Collagen quantification in recovered culture medium. IMR90 fibroblasts were cultured embedded in PLMA hydrogels and supplemented with ascorbic acid and TGF- $\beta$  for 48h. Soluble collagen was extracted and measured using Sircol Assay kit. Preliminary results (n=1).

Observing the morphology and behavior of cultured fibroblasts in each PLMA100 concentration, we suggest that PLMA100 hydrogels at 15% and 20% w/v have fibrotic-specific mechanics and regulatory cues relevant to study human fibrotic lung diseases, while PLMA100 hydrogels at 10% w/v approximate to the physiological stiffness of healthy human lungs, and that their compliance appears to protect against fibroblast activation and myodifferentiation, even in the presence of exogenous profibrotic cues (TGF- $\beta$ ). These results are in agreement with previous evidence that showed the regulatory role of ECM in the activation and myodifferentiation of fibroblasts *in vitro*<sup>93,94</sup>. Liu and colleagues found that fibroblasts cultured on polyacrylamide-crosslinked hydrogels maintained a quiescent phenotype at low substrate rigidity (0.1-3kPa), while stiffer hydrogels (20-50kPa) triggered fibroblast activation, which was manifested by spindle-like shaped fibroblasts accumulated and aligned in parallel swirls<sup>10</sup>. They also investigated the regulation of fibroblast matrix synthesis by substrate stiffness and results demonstrated a gradual increase of procollagen I protein expression in cells with increased stiffness along with decreases in gene expression of MMP1, a collagenolytic enzyme. Procollagen I synthesis was enhanced with supplementation of culture medium with TGF- $\beta$ 1 for 3 days across the entire stiffness gradient, which suggests a cooperative role of both soluble profibrotic factors and mechanical signals to enhance matrix synthesis<sup>10</sup>.

## Bibliography:

1. Bagnato, G. & Harari, S. Cellular interactions in the pathogenesis of interstitial lung diseases. *European Respiratory Review* **24**, 102–114 (2015).
2. Fiore, V. F. *et al.*  $\alpha_v\beta_3$  Integrin drives fibroblast contraction and strain stiffening of soft provisional matrix during progressive fibrosis. *JCI Insight* **3**, (2018).
3. Chong, D. L. W. *et al.* S49 The role of platelet-derived TGF $\beta$  in pulmonary fibrosis. *Thorax* **71**, A30–A30 (2016).
4. Cahill, E. F., Kennelly, H., Carty, F., Mahon, B. P. & English, K. Hepatocyte Growth Factor Is Required for Mesenchymal Stromal Cell Protection Against Bleomycin-Induced Pulmonary Fibrosis. *STEM CELLS Translational Medicine* **5**, 1307–1318 (2016).
5. Doyle, A. D. & Yamada, K. M. Mechanosensing via cell-matrix adhesions in 3D microenvironments. *Experimental Cell Research* **343**, 60–66 (2016).
6. Raab, M., Shin, J.-W. & Discher, D. E. Matrix elasticity in vitro controls muscle stem cell fate in vivo. *Stem Cell Res Ther* **1**, 38 (2010).
7. Nestor, C. E. *et al.* Rapid reprogramming of epigenetic and transcriptional profiles in mammalian culture systems. *Genome Biology* **16**, 11 (2015).
8. Balestrini, J. L., Chaudhry, S., Sarrazy, V., Koehler, A. & Hinz, B. The mechanical memory of lung myofibroblasts. *Integrative Biology* **4**, 410–421 (2012).
9. Tse, J. R. & Engler, A. J. Preparation of Hydrogel Substrates with Tunable Mechanical Properties. *Current Protocols in Cell Biology* **47**, 10.16.1-10.16.16 (2010).
10. Liu, F. *et al.* Feedback amplification of fibrosis through matrix stiffening and COX-2 suppression. *Journal of Cell Biology* **190**, 693–706 (2010).
11. Chung, K.-P. *et al.* Mitofusins regulate lipid metabolism to mediate the development of lung fibrosis. *Nature Communications* **10**, 3390 (2019).
12. Laucho-Contreras, M. E., Polverino, F., Rojas-Quintero, J., Wang, X. & Owen, C. A. Club cell protein 16 (Cc16) deficiency increases inflamm-aging in the lungs of mice. *Physiological Reports* **6**, e13797 (2018).
13. Nureki, S.-I. *et al.* Expression of mutant *Sftpc* in murine alveolar epithelia drives spontaneous lung fibrosis. *J Clin Invest* **128**, 4008–4024 (2018).

14. Sundarakrishnan, A., Chen, Y., Black, L. D., Aldridge, B. B. & Kaplan, D. L. Engineered cell and tissue models of pulmonary fibrosis. *Advanced Drug Delivery Reviews* **129**, 78–94 (2018).
15. Kendall, R. T. & Feghali-Bostwick, C. A. Fibroblasts in fibrosis: novel roles and mediators. *Front. Pharmacol.* **5**, (2014).
16. Noble, P. W., Barkauskas, C. E. & Jiang, D. Pulmonary fibrosis: patterns and perpetrators. *J Clin Invest* **122**, 2756–2762 (2012).
17. King, T. E., Pardo, A. & Selman, M. Idiopathic pulmonary fibrosis. *Lancet* **378**, 1949–1961 (2011).
18. Marchand-Adam, S. *et al.* Defect of pro-hepatocyte growth factor activation by fibroblasts in idiopathic pulmonary fibrosis. *Am J Respir Crit Care Med* **174**, 58–66 (2006).
19. Geng, Y. *et al.* PD-L1 on invasive fibroblasts drives fibrosis in a humanized model of idiopathic pulmonary fibrosis. *JCI Insight* **4**,.
20. Li, Y. *et al.* Severe lung fibrosis requires an invasive fibroblast phenotype regulated by hyaluronan and CD44. *Journal of Experimental Medicine* **208**, 1459–1471 (2011).
21. Wohlfahrt, T. *et al.* PU.1 controls fibroblast polarization and tissue fibrosis. *Nature* **566**, 344–349 (2019).
22. Bagalad, B. S., Mohan Kumar, K. P. & Puneeth, H. K. Myofibroblasts: Master of disguise. *J Oral Maxillofac Pathol* **21**, 462–463 (2017).
23. Pakshir, P. & Hinz, B. The big five in fibrosis: Macrophages, myofibroblasts, matrix, mechanics, and miscommunication. *Matrix Biol.* **68–69**, 81–93 (2018).
24. Van De Water, L., Varney, S. & Tomasek, J. J. Mechanoregulation of the Myofibroblast in Wound Contraction, Scarring, and Fibrosis: Opportunities for New Therapeutic Intervention. *Adv Wound Care (New Rochelle)* **2**, 122–141 (2013).
25. Li, B. & Wang, J. H.-C. Fibroblasts and Myofibroblasts in Wound Healing: Force Generation and Measurement. *J Tissue Viability* **20**, 108–120 (2011).
26. Biernacka, A., Dobaczewski, M. & Frangogiannis, N. G. TGF- $\beta$  signaling in fibrosis. *Growth Factors* **29**, 196–202 (2011).
27. Saito, A., Horie, M. & Nagase, T. TGF- $\beta$  Signaling in Lung Health and Disease. *Int J Mol Sci* **19**, (2018).

28. Barcellos-Hoff, M. H., Derynck, R., Tsang, M. L. & Weatherbee, J. A. Transforming growth factor-beta activation in irradiated murine mammary gland. *J Clin Invest* **93**, 892–899 (1994).
29. Hinz, B. The extracellular matrix and transforming growth factor- $\beta$ 1: Tale of a strained relationship. *Matrix Biology* **47**, 54–65 (2015).
30. Annes, J. P., Munger, J. S. & Rifkin, D. B. Making sense of latent TGFbeta activation. *J Cell Sci* **116**, 217–224 (2003).
31. Ignatz, R. A. & Massagué, J. Transforming growth factor-beta stimulates the expression of fibronectin and collagen and their incorporation into the extracellular matrix. *J Biol Chem* **261**, 4337–4345 (1986).
32. Lyons, R. M., Keski-Oja, J. & Moses, H. L. Proteolytic activation of latent transforming growth factor-beta from fibroblast-conditioned medium. *J Cell Biol* **106**, 1659–1665 (1988).
33. Gabbiani, G. The myofibroblast in wound healing and fibrocontractive diseases. *The Journal of Pathology* **200**, 500–503 (2003).
34. P, K. *et al.* Endothelin-1 and transforming growth factor-beta1 independently induce fibroblast resistance to apoptosis via AKT activation. *Am J Respir Cell Mol Biol* **41**, 484–493 (2009).
35. Willis, B. C. *et al.* Induction of epithelial-mesenchymal transition in alveolar epithelial cells by transforming growth factor-beta1: potential role in idiopathic pulmonary fibrosis. *Am J Pathol* **166**, 1321–1332 (2005).
36. Drakopanagiotakis, F., Xifteri, A., Polychronopoulos, V. & Bouros, D. Apoptosis in lung injury and fibrosis. *European Respiratory Journal* **32**, 1631–1638 (2008).
37. C, K. & Ja, M. The roles of the myofibroblast in idiopathic pulmonary fibrosis. Ultrastructural and immunohistochemical features of sites of active extracellular matrix synthesis. *Am J Pathol* **138**, 1257–1265 (1991).
38. Nurden, A. T., Nurden, P., Sanchez, M., Andia, I. & Anitua, E. Platelets and wound healing. *Front. Biosci.* **13**, 3532–3548 (2008).
39. Amaral, R. J. F. C. do & Balduino, A. Platelets in Tissue Regeneration. *The Non-Thrombotic Role of Platelets in Health and Disease* (2015) doi:10.5772/61184.
40. Etulain, J. Platelets in wound healing and regenerative medicine. *Platelets* **29**, 556–568 (2018).

41. Sut, C. *et al.* The Non-Hemostatic Aspects of Transfused Platelets. *Front. Med.* **5**, (2018).
42. Barsotti, M. C. *et al.* Fibrin acts as biomimetic niche inducing both differentiation and stem cell marker expression of early human endothelial progenitor cells. *Cell Prolif* **44**, 33–48 (2010).
43. Ahmed, T. A. E., Griffith, M. & Hincke, M. Characterization and Inhibition of Fibrin Hydrogel–Degrading Enzymes During Development of Tissue Engineering Scaffolds. *Tissue Engineering* **13**, 1469–1477 (2007).
44. Ye, Q. *et al.* Fibrin gel as a three dimensional matrix in cardiovascular tissue engineering. *Eur J Cardiothorac Surg* **17**, 587–591 (2000).
45. Yuan Ye, K., Sullivan, K. E. & Black, L. D. Encapsulation of cardiomyocytes in a fibrin hydrogel for cardiac tissue engineering. *J Vis Exp* (2011) doi:10.3791/3251.
46. Jockenhoevel, S. *et al.* Fibrin gel -- advantages of a new scaffold in cardiovascular tissue engineering. *Eur J Cardiothorac Surg* **19**, 424–430 (2001).
47. Thomson, K. S. *et al.* Prevascularized microtemplated fibrin scaffolds for cardiac tissue engineering applications. *Tissue Eng Part A* **19**, 967–977 (2013).
48. Birla, R. K., Borschel, G. H., Dennis, R. G. & Brown, D. L. Myocardial engineering in vivo: formation and characterization of contractile, vascularized three-dimensional cardiac tissue. *Tissue Eng.* **11**, 803–813 (2005).
49. Wittmann, K. *et al.* Engineering Vascularized Adipose Tissue Using the Stromal-Vascular Fraction and Fibrin Hydrogels. *Tissue Engineering Part A* **21**, 1343–1353 (2015).
50. Soleimannejad, M. *et al.* Fibrin gel as a scaffold for photoreceptor cells differentiation from conjunctiva mesenchymal stem cells in retina tissue engineering. *Artificial Cells, Nanomedicine, and Biotechnology* **46**, 805–814 (2018).
51. Soleimannejad, M. *et al.* Retina tissue engineering by conjunctiva mesenchymal stem cells encapsulated in fibrin gel: Hypotheses on novel approach to retinal diseases treatment. *Medical Hypotheses* **101**, 75–77 (2017).
52. Gandhi, J. K. *et al.* Fibrin hydrogels as a xenofree and rapidly degradable support for transplantation of retinal pigment epithelium monolayers. *Acta Biomaterialia* **67**, 134–146 (2018).
53. Gholobova, D. *et al.* Endothelial Network Formation Within Human Tissue-Engineered Skeletal Muscle. *Tissue Engineering Part A* **21**, 2548–2558 (2015).

54. Wang, X. & Liu, C. Fibrin Hydrogels for Endothelialized Liver Tissue Engineering with a Predesigned Vascular Network. *Polymers (Basel)* **10**, (2018).
55. Maja Popovic *et al.* FIBRIN GEL AS A SCAFFOLD FOR SKIN SUBSTITUTE - PRODUCTION AND CLINICAL EXPERIENCE. **55**, 279–289 (2016).
56. Eyrich, D. *et al.* Long-term stable fibrin gels for cartilage engineering. *Biomaterials* **28**, 55–65 (2007).
57. Noori, A., Ashrafi, S. J., Vaez-Ghaemi, R., Hatamian-Zaremi, A. & Webster, T. J. A review of fibrin and fibrin composites for bone tissue engineering. *Int J Nanomedicine* **12**, 4937–4961 (2017).
58. Ahmed, T. A. E., Dare, E. V. & Hincke, M. Fibrin: A Versatile Scaffold for Tissue Engineering Applications. *Tissue Engineering Part B: Reviews* **14**, 199–215 (2008).
59. Gamboa-Martínez, T. C., Luque-Guillén, V., González-García, C., Gómez Ribelles, J. L. & Gallego-Ferrer, G. Crosslinked fibrin gels for tissue engineering: Two approaches to improve their properties: Crosslinked Fibrin Gels for Tissue Engineering. *J. Biomed. Mater. Res.* **103**, 614–621 (2015).
60. Martínez-Zapata, M. J. *et al.* Efficacy and safety of the use of autologous plasma rich in platelets for tissue regeneration: a systematic review. *Transfusion* **49**, 44–56 (2009).
61. Lang, S., Loibl, M. & Herrmann, M. Platelet-Rich Plasma in Tissue Engineering: Hype and Hope. *ESR* **59**, 265–275 (2018).
62. Giusti, I., D’Ascenzo, S., Macchiarelli, G. & Dolo, V. In vitro evidence supporting applications of platelet derivatives in regenerative medicine. *Blood Transfusion* **18**, 117–129 (2020).
63. World Health Organization. Guidelines on good manufacturing practices for blood establishments. *WHO Technical Report Series* 148–214 (2011).
64. European Directorate for the Quality of Medicines & Healthcare. *Guide to the preparation, use and quality assurance of blood components: recommendation No. R (95) 15.* (2017).
65. Pallotta, I. *et al.* Characteristics of platelet gels combined with silk. *Biomaterials* **35**, 3678–3687 (2014).
66. Fekete, N. *et al.* Platelet lysate from whole blood-derived pooled platelet concentrates and apheresis-derived platelet concentrates for the isolation and expansion of human bone marrow mesenchymal stromal cells: production process, content and identification of active components. *Cytotherapy* **14**, 540–554 (2012).

67. Lischer, M. *et al.* Human platelet lysate stimulated adipose stem cells exhibit strong neurotrophic potency for nerve tissue engineering applications. *Regenerative Medicine* **15**, 1399–1408 (2020).
68. Monteiro, C., Santos, S., Custodio, C. & Mano, J. F. Human Platelet Lysates-Based Hydrogels: A Novel Personalized 3D Platform for Spheroid Invasion Assessment. *Advanced Science* **7**, 1902398 (2020).
69. Santos, S. C., Custódio, C. A. & Mano, J. F. Photopolymerizable Platelet Lysate Hydrogels for Customizable 3D Cell Culture Platforms. *Advanced Healthcare Materials* **7**, 1800849 (2018).
70. Moroz, A., Bittencourt, R. A. C., Almeida, R. P., Felisbino, S. L. & Deffune, E. Platelet lysate 3D scaffold supports mesenchymal stem cell chondrogenesis: An improved approach in cartilage tissue engineering. *Platelets* **24**, 219–225 (2013).
71. Copland, I. B., Garcia, M. A., Waller, E. K., Roback, J. D. & Galipeau, J. The effect of platelet lysate fibrinogen on the functionality of MSCs in immunotherapy. *Biomaterials* **34**, 7840–7850 (2013).
72. Fortunato, T. M., Beltrami, C., Emanuelli, C., De Bank, P. A. & Pula, G. Platelet lysate gel and endothelial progenitors stimulate microvascular network formation in vitro : tissue engineering implications. *Scientific Reports* **6**, 25326 (2016).
73. Altaie, A., Owston, H. & Jones, E. Use of platelet lysate for bone regeneration - are we ready for clinical translation? *World J Stem Cells* **8**, 47–55 (2016).
74. Bessonov, I. V. *et al.* Fabrication of hydrogel scaffolds via photocrosslinking of methacrylated silk fibroin. *Biomed. Mater.* **14**, 034102 (2019).
75. Asano, S. *et al.* Matrix stiffness regulates migration of human lung fibroblasts. *Physiol Rep* **5**, (2017).
76. Freeberg, M. A. T. *et al.* Mechanical Feed-Forward Loops Contribute to Idiopathic Pulmonary Fibrosis. *The American Journal of Pathology* **191**, 18–25 (2021).
77. Santos, A. & Lagares, D. Matrix Stiffness: the Conductor of Organ Fibrosis. *Curr Rheumatol Rep* **20**, 2 (2018).
78. Gross, T. J. & Hunninghake, G. W. Idiopathic pulmonary fibrosis. *N Engl J Med* **345**, 517–525 (2001).

79. Kuhn, C. & McDonald, J. A. The roles of the myofibroblast in idiopathic pulmonary fibrosis. Ultrastructural and immunohistochemical features of sites of active extracellular matrix synthesis. *Am J Pathol* **138**, 1257–1265 (1991).
80. Kim, U.-J., Park, J., Joo Kim, H., Wada, M. & Kaplan, D. L. Three-dimensional aqueous-derived biomaterial scaffolds from silk fibroin. *Biomaterials* **26**, 2775–2785 (2005).
81. Kim, H. J., Kim, U.-J., Vunjak-Novakovic, G., Min, B.-H. & Kaplan, D. L. Influence of macroporous protein scaffolds on bone tissue engineering from bone marrow stem cells. *Biomaterials* **26**, 4442–4452 (2005).
82. Choi, D. J. *et al.* Effect of the pore size in a 3D bioprinted gelatin scaffold on fibroblast proliferation. *Journal of Industrial and Engineering Chemistry* **67**, 388–395 (2018).
83. Mandal, B. B. & Kundu, S. C. Cell proliferation and migration in silk fibroin 3D scaffolds. *Biomaterials* **30**, 2956–2965 (2009).
84. Mygind, T. *et al.* Mesenchymal stem cell ingrowth and differentiation on coralline hydroxyapatite scaffolds. *Biomaterials* **28**, 1036–1047 (2007).
85. Annabi, N. *et al.* Controlling the Porosity and Microarchitecture of Hydrogels for Tissue Engineering. *Tissue engineering. Part B, Reviews* **16**, 371–83 (2010).
86. Loh, Q. L. & Choong, C. Three-Dimensional Scaffolds for Tissue Engineering Applications: Role of Porosity and Pore Size. *Tissue Eng Part B Rev* **19**, 485–502 (2013).
87. Choi, J. R., Yong, K. W., Choi, J. Y. & Cowie, A. C. Recent advances in photo-crosslinkable hydrogels for biomedical applications. *BioTechniques* **66**, 40–53 (2019).
88. Grinnell, F. Fibroblast biology in three-dimensional collagen matrices. *Trends in Cell Biology* **13**, 264–269 (2003).
89. White, E. S. Lung Extracellular Matrix and Fibroblast Function. *Annals ATS* **12**, S30–S33 (2015).
90. Discher, D. E., Janmey, P. & Wang, Y.-L. Tissue cells feel and respond to the stiffness of their substrate. *Science* **310**, 1139–1143 (2005).
91. Arnaout, M. A., Goodman, S. L. & Xiong, J.-P. Structure and mechanics of integrin-based cell adhesion. *Curr Opin Cell Biol* **19**, 495–507 (2007).



92. Branco da Cunha, C. *et al.* Influence of the stiffness of three-dimensional alginate/collagen-I interpenetrating networks on fibroblast biology. *Biomaterials* **35**, 8927–8936 (2014).
93. Huang, X. *et al.* Matrix Stiffness–Induced Myofibroblast Differentiation Is Mediated by Intrinsic Mechanotransduction. *Am J Respir Cell Mol Biol* **47**, 340–348 (2012).
94. Booth, A. J. *et al.* Acellular normal and fibrotic human lung matrices as a culture system for in vitro investigation. *Am J Respir Crit Care Med* **186**, 866–876 (2012).

# **Chapter IV**

## **Conclusions and Future Perspectives**

## Conclusions and Future Perspectives

Lung fibroblasts adhered to PLMA100 hydrogels, adopting different morphologies as matrix stiffness changed, without compromising cell viability. Also, they participated in matrix rearrangements within PLMA100 hydrogels at 15% and 20% w/v. These findings suggest that increased matrix stiffness support disease-like phenotype of cultured lung fibroblasts, and that by altering matrix stiffness we can modulate fibrosis progression. These humanized 3D hydrogels could provide the means to investigate the mechanistic contribution of the ECM to fibrotic lung disease pathogenesis. Furthermore, by changing the degree of methacrylation or concentration of PLMA hydrogels, we could adapt this 3D cell culture platform to model other human organs or conditions in order to enhance the translatability of TE research.

In the future, further investigations should be considered to support that matrix stiffness triggers a disease-phenotype in fibroblasts, as no fibrosis-specific markers of fibroblast activation and myodifferentiation were measured. Besides comparing fibroblasts morphology and matrix synthesis capacity in matrices with different stiffnesses, we should evaluate the expression of fibroblast activation markers, such as secreted TGF- $\beta$  and bFGF, and also the expression of fibroblast myodifferentiation markers, such as  $\alpha$ -SMA, and COL1 $\alpha$ 1, which are usually upregulated in myofibroblasts in response to profibrotic agents such as TGF- $\beta$ . In fact, another idea is to evaluate collagen synthesis by cells in PLMA100 hydrogels without the profibrotic stimulation of TGF- $\beta$ , considering that research shows that fibroblast myodifferentiation in the absence of TGF- $\beta$  signaling can be triggered simply by altering the stiffness of their substrate.

In this work, we focused mainly on matrices that recapitulated the pathological stiffness of fibrotic tissue (PLMA100 at 15% and 20% w/v). Considering that fibrotic lung diseases are characterized by progressive lung tissue stiffening, perhaps we could consider using a more compliant hydrogel (PLMA100 at 10% w/v) which models healthy lung tissue, and then add cues (e.g., profibrotic agents such as TGF- $\beta$ ) to direct tissue development towards a fibrotic phenotype, therefore allowing a temporal control over fibrogenesis. This would possibly allow the replication of different stages of lung fibrosis, and therefore a deeper understanding of disease progression.

Finally, the model herein presented lack the multicellular organization found in native fibrotic tissues, particularly epithelial, endothelial, and immune cells, that, together with the mesenchymal compartment, play key roles in wound healing responses, and therefore in fibrosis. Nevertheless,

PLMA100 hydrogels could be co-cultured with other cells in order to mimic organ-specific multicellular responses, therefore better recapitulating lung tissue physiology.